


RESEARCH ARTICLE

Open Access



Ensemble rainfall–runoff and inundation simulations using 100 and 1000 member rainfalls by 4D LETKF on the Kumagawa River flooding 2020

Kenichiro Kobayashi^{1*} , Le Duc², Takuya Kawabata³, Atsushi Tamura⁴, Tsutao Oizumi³, Kazuo Saito⁵, Daisuke Nohara⁶ and Tetsuya Sumi⁷

Abstract

This paper presents the 1000 ensemble flood simulations using ensemble rainfalls simulated by 4D LETKF. The number of ensemble rainfall members is large as 1000 compared to the operational rainfall products of two-digit numbers to avoid sampling errors in the three-dimensional meteorological simulation based on chaotic theory. Using the large data set, 1000 ensemble rainfall–runoff for dam catchments and high-resolution inundation simulations of large area are carried out focusing on the Kumagawa river catchment. Herewith, the comparisons were carried out with 21-member ensemble rainfalls of an operational forecast by Japan Meteorological Agency and 100-member 4D-LETKF ensemble rainfalls simulated independent of 1000-member 4D-LETKF. At the same time, the accuracy of selective 100-member ensembles out of 1000 members is investigated. As a result, although many previous research works show a large number of ensemble simulations are necessary for three-dimensional meteorological field, the number could be reduced in the catchment-average rainfall–runoff and 2.5-dimensional inundation simulations given that the rainfall prediction has a certain level of accuracy since improving the discharge prediction accuracy with lower dimension is sometimes possible by adjusting the horizontally/vertically integrated model parameters determined by topography and soil characteristics in advance against the observed rainfall. Also, the 1000 ensembles could be classified into several patterns in horizontally accumulated 2D rainfall field. Likewise, the flood flow moves toward the low elevation area and river; thus, the resultant 2.5-dimensional flood field does not show much variety as three-dimensional meteorological simulation. The paper summarizes these studies.

Keywords 1000 Ensemble, 4D LETKF, Rainfall–runoff, Storage function model, Inundation, Shallow water equation, Kumagawa River

*Correspondence:

Kenichiro Kobayashi
kkobayashi@phoenix.kobe-u.ac.jp

¹ Research Center for Urban Safety and Security, Kobe University, Kobe, Japan

² Institute of Engineering Innovation, The University of Tokyo, Tokyo, Japan

³ Meteorological Research Institute, Tsukuba, Japan

⁴ Department of Civil Engineering, Kobe University, Kobe, Japan

⁵ Atmosphere and Ocean Research Institute, The University of Tokyo, Kashiwa, Chiba, Japan

⁶ Sustainable Society Laboratory, Kajima Technical Research Institute, Chofu, Japan

⁷ Disaster Prevention Research Institute, Kyoto University, Kyoto, Japan



© The Author(s) 2023. **Open Access** This article is licensed under a Creative Commons Attribution 4.0 International License, which permits use, sharing, adaptation, distribution and reproduction in any medium or format, as long as you give appropriate credit to the original author(s) and the source, provide a link to the Creative Commons licence, and indicate if changes were made. The images or other third party material in this article are included in the article's Creative Commons licence, unless indicated otherwise in a credit line to the material. If material is not included in the article's Creative Commons licence and your intended use is not permitted by statutory regulation or exceeds the permitted use, you will need to obtain permission directly from the copyright holder. To view a copy of this licence, visit <http://creativecommons.org/licenses/by/4.0/>.

1 Introduction

Numerical weather predictions (NWP) are the only way for quantitative weather forecasting and the necessity of predicting future weather accurately is increasing due to increasing weather-related disasters by realizing global warming. However, NWP) have inherent errors, since (1) there are errors in the initial/boundary conditions due to a lack of perfect observations representing the actual atmosphere; and (2) the governing equation of the numerical weather model itself is not perfect due to lack of knowledge (Japan Meteorological Agency: JMA 2021). Even if errors in the initial condition are very small, the NWP in the long future would result in unrealistic predictions, which is known as the chaotic nature of the atmosphere.

To estimate the errors in NWP) s, ensemble prediction systems (EPS) are gaining more attention nowadays. It is widely thought that spreads of EPSs, which consist of several model runs, represent errors in the predictions. To incorporate these spreads of prediction variations, global and mesoscale ensemble weather prediction systems-GEPS (Yamaguchi et al. 2021) and MEPS (Ono et al. 2021), respectively, are in operation now in Japan. The specifications of GEPS and MEPS are given in Table 1 along with the global ensemble prediction system (ENS) by ECMWF. The usefulness of GEPS, MEPS as well as ENS ECMWF is now shown by many stakeholders in Japan, not only for weather prediction but also for flood prediction including statistical post-processing and AI applications (Kobayashi et al. 2016a, b; Sayama et al. 2020; Nohara and Sumi 2020; Nohara et al. 2022; Hanasaki 2019).

On the other hand, the point we are paying attention to in this paper is that the number of ensemble members in MEPS is 21, which is modest. However, the consideration is becoming more prevalent that the number of ensemble members must be much greater to fulfill the probability distribution of the ensemble simulations to avoid sampling error. Especially in ensemble data assimilation, increasing the number of ensemble members is necessary to be more precise, which helps the estimation of the errors owing to decreasing the sampling errors. In this context, the research for mesoscale weather mega

ensembles can be found in Kawabata and Ueno (2020), Kunii (2014), Necker et al. (2020), Duc and Saito (2017), Duc et al. (2021) all with more than 1000 members.

Kawabata and Ueno (2020) investigated the non-Gaussianity of the cumulonimbus prediction with 2 km and 1000 members and found the non-Gaussianity was initiated in the updraft at low troposphere. Kunii (2014) dealt with 1000 members with a 15-km resolution and illustrated that sampling errors in the background covariances significantly reduced in comparison with a 100-member ensemble, and concluded that an ensemble size larger than 500 is enough large to approximate the covariances. Necker et al. (2020) compared a 1000-member ensemble with a 15-km resolution by the Japanese numerical weather model SCALE and a 40-member ensemble by COSMO from the German Weather Service, and they found that sampling errors in background error covariances reduced in the 1000-member ensemble. The research aims of the above all experiments focus mostly on sampling errors and Gaussianity in errors and do not show their performances in precipitation predictions, even more in flood predictions.

On the other hand, the research also considering the ensemble flood simulation driven by the 1600-member ensemble weather predictions (Duc and Saito 2017) can be found in Kobayashi et al. (2019, 2020). This was an initial work on probability flood forecasting using a physically based distributed rainfall-runoff model and a huge number of ensemble rainfall forecasts obtained from a four-dimensional variational ensemble assimilation system. They showed that the probabilistic consideration in the real sense with huge 1600-member ensembles was possible along with the significant improvement in rainfall and flood simulations. Likewise, the result succeeded in indicating the necessity of emergency flood operations with enough lead times and probabilities. They also discussed the difficulty of selecting the best ensemble members due to the nonlinearity of the weather.

Recently, Duc et al. (2021) carried out 1000 ensemble weather simulations targeting July 2020 Kyushu heavy rain. Since the event brought extreme damage to flooded areas, they designed the experiment for predicting heavy rain, which is described in Duc et al. (2021), as well as the

Table 1 Specification of GEPS, MEPS and global ensemble (ENS) by ECMWF

| | GEPS | MEPS | ENS by ECMWF |
|------------------------------|------------------------------------|-----------------------|---------------|
| Resolution | Approx. 40 km | 5 km | 18 km |
| Number of prediction per day | 4 (00, 06, 12, 18UTC) | 4 (00, 06, 12, 18UTC) | 2 (00, 12UTC) |
| Duration of the prediction | 132 (06, 18UTC) 264 (00, 12UTC) | 39 | 360 |
| Number of ensembles | 27 | 21 | 51 |

flood event. Thus, these 1000-member ensemble weather simulations are used for the ensemble flood simulations of this paper whose overview is explained later. Overall, this paper attempted to carry out 1000 ensemble flood simulations driven by the 1000 ensemble weather simulations using a lumped rainfall–runoff model with a Kalman filter, and flood simulations with a shallow water equation, which has different aspects from Kobayashi et al. (2019) using a physically based distributed rainfall–runoff model. The scientific question in the paper is that in meteorology we have high uncertainty in rainfall forecasts based on chaotic nature, and this requires a large number of ensemble members. However, in flood forecasting of hydrology, given that the rainfall prediction has a certain level accuracy, it is not necessarily true because certain factors like topography and river networks determine the flow movement very much, thus may reduce uncertainties in flood forecasting compared to weather forecasting. The large number may only be important for long lead times. The paper attempted to answer this scientific question.

The basic attempts of this paper are: (1) fixing the parameters of the rainfall–runoff and inundation model using the radar–raingauge rainfall distribution data by JMA (hereafter R/A) as observation and (2) investigating the variations/uncertainties of the flood predictions mainly due to the uncertainties of ensemble weather simulations only, then (3) estimating the rainfall–runoff model state variables to minimize the effect of the runoff model uncertainties using a Kalman filter. This is due to the fact that, in general, state variables of runoff models must be adjusted even against quasi-perfect rainfalls (i.e., R/A) at each different rainfall event.

It is noted that Oizumi et al. (2022) also currently carry out 1000 ensemble flood simulation using Japan Meteorological Agency operational Runoff-Index Model, a rainfall–runoff model different from this paper using the same 1000 ensemble rainfall data set. However, the purpose and focus are different from this paper.

The structure of the rest of this paper is as follows. Section 2.1 presents a brief description of the 1000 ensemble rainfalls used in the paper. Section 2.2 explains the Kumagawa river catchment, the target river basin in this paper. Section 2.3 shows the flood simulation conditions with a rainfall–runoff model and a shallow water equation model. Sections 3.1–3.2 show the results of 1000 ensemble rainfall–runoff simulation for the Ichifusa dam catchment. Likewise, Sect. 3.3–3.4 shows the results for the Kawabegawa dam catchment. Section 3.5 shows the result of 1000 inundation simulations. Section 3.6 presents the application of a Kalman filter on the rainfall–runoff simulations. Finally, Chapter 4 states the concluding remarks and future aspects.

2 Methods/experimental

2.1 High-resolution ensemble precipitation forecasts

In order to provide rainfall forecasts for the hydrological model, three ensemble prediction systems (EPS) are used. The first EPS is the operational mesoscale ensemble prediction system (MEPS) running at JMA with 21 ensemble members. The other two EPSs are conducted by Duc et al. (2021) using the JMA nonhydrostatic model (NHM) and the local ensemble transform Kalman filter (LETKF) to generate initial perturbations. The data assimilation system NHM-LETKF is described in Duc et al. (2015). All settings of these two EPSs are identical except the number of ensemble members, which are 100 and 1000. Thus, by using the three EPSs, we can examine the impact of the number of ensemble members on the uncertainty quantification of rainfall and flood predictions.

NHM-LETKF run with dual resolutions: a low-resolution grid with 15-km grid spacing for analysis perturbations and a high-resolution grid with 5-km grid spacing for analyses. The analysis domain is copied from the JMA's operational domain, which is much larger than the forecast domain [see Fig. 2 of Duc et al. (2021)]. Except for radiances and rain analyses, they assimilate the same observations that are assimilated into the JMA's operational data assimilation system ASUCA-VAR. The boundary conditions and boundary perturbations are obtained from the JMA's global forecasts. The assimilating run with 1000 ensemble members is relatively challenging because huge computational costs are involved. In order to reduce the computational cost, they turn off vertical localization in NHM-LETKF. Duc et al. (2021) point out that removing vertical localization indeed has a positive impact on the heavy rain forecast in Kyushu.

The forecast domain is a 2-km grid-spacing domain centered at Kyushu. This domain has 819×715 horizontal grid points and 60 vertical levels. The boundary conditions are interpolated from the JMA's global forecasts. The boundary perturbations are extracted from the JMA's 1-week global ensemble forecasts. All ensemble members start at 18 JST July 3rd 2020 and run for 24-h forecasts. Note that the forecast domain of MEPS is the same as the analysis domain of NHM-LETKF with the grid spacing of 5 km.

For illustration, Fig. 1 shows the deterministic and probabilistic precipitation forecasts from the 1000-member EPS in comparison with the observations at the peak period 00–09 JST of the July 2020 Kyushu heavy rain (July 4th). Clearly, these forecasts succeed in predicting both the rainfall location and the rainfall amount. In order to quantify this subjective evaluation, Fig. 2 plots the Fractions Skill Score (FSS) (Roberts and Lean 2008) calculated for the 3-h deterministic precipitation forecasts over Kyushu. This figure also displays

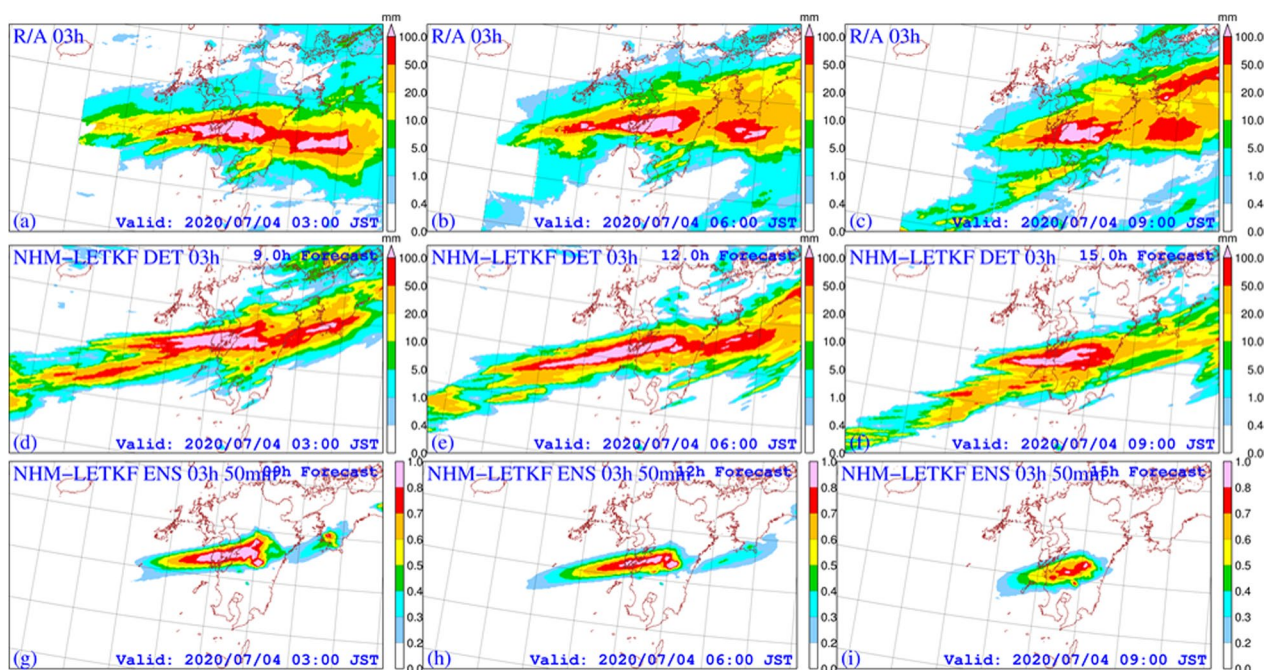


Fig. 1 a, b, c Observations of consecutive 3-h precipitations between 00 and 09 JST July 4th 2020. d, e, f The corresponding 2-km forecasts by NHM-LETKF started at 18 JST July 4th 2020. g, h, i The corresponding 2-km probabilistic forecasts with respect to a rainfall threshold of 50 mm/3 h. (Reproduced Duc et al. 2021)

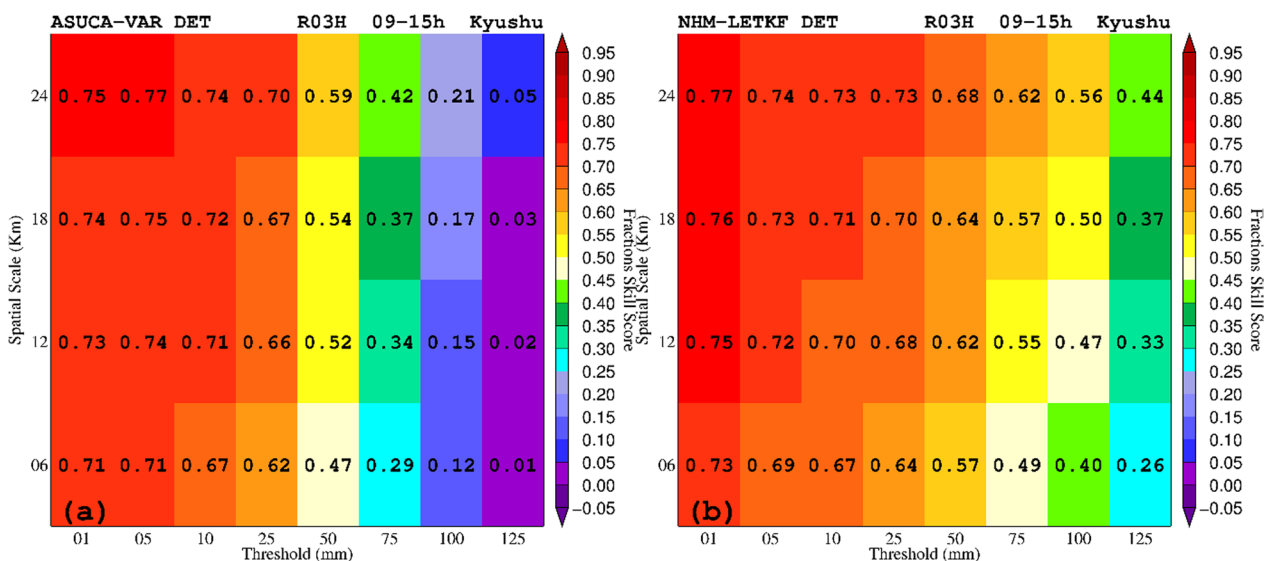


Fig. 2 FSSs of the consecutive 3-h precipitations forecasted by ASUCA-VAR and NHM-LETKF against the R/A observations between 00 and 09 JST July 4th 2020 over the Kumagawa catchment. (Reproduced Duc et al. 2021)

the FSSs of the downscaling forecasts from the JMA's ASUCA-VAR analysis at 2-km grid spacing for comparison. It can be seen that the NHM-LETKF forecasts even beat the operational forecasts in this case. Thus, it can be expected that NHM-LETKF will yield good

precipitation forecasts for the Kumagawa catchment. This is indeed the case as verified in Fig. 3 in which the evolutions of the accumulated rainfall, averaged over this area, are presented.

2.2 Kumagawa river catchment

Receiving the three rainfall ensemble forecasts, this paper presents its application to flood simulations of the Kumagawa river catchment. Figure 4 shows the Kumagawa river catchment (catchment area: 1765 km²). The river experienced the largest-ever flooding on July 4, 2020. The total accumulated rainfall at the Hitoyoshi rainfall observatory (Fig. 4) attained 420 mm between 00JST July 3 and 24JST July 4. Note that the average rainfall of July in the Hitoyoshi rainfall observatory was 471.4 mm. The hourly rainfall over 30 mm continued for 8 h having a line shape rainfall band from the predawn of July 4. At Taragi and Hitoyoshi rainfall observatories (Fig. 4), the 6-, 12- and 24-h rainfalls exceeded the historical records of July in 1965 and 1982 (Fukuoka district meteorological observatory 2020; The Kinki district of maintenance station, Ministry of Land, Infrastructure, Transport and Tourism 2020).

In Fig. 4, the catchment area of the already existing Ichifusa dam is shown. The catchment area is 158 km². The discharge into the Ichifusa dam was simulated using a lumped rainfall–runoff model (hereafter RRM) or the storage function model (hereafter SFM). The Kawabegawa dam (catchment area 470 km²) is in the planning stage, though the catchment area is shown also in Fig. 4 since the ensemble discharges at the site were also estimated using the RRM. Figure 4 also shows the nested computational area with a resolution of 5 m. The flood simulation using a shallow water equation (hereafter SWE) was carried out in the nested computational area. The outflows from Ichifusa and Kawabegawa dams

were provided to the flood simulation by SWE; then, the propagation of the river flows including overtopping was simulated. At the same time, R/A was provided over the entire nested computational area. Thus, the inland flooding by the rainfall as well as the river flows by the two discharge inputs from the dams is simultaneously simulated.

The red color polygon in Fig. 4 shows the inundated area (i.e., flood mark) by the Geospatial Information Authority of Japan (hereafter GSI). The simulated flooding for the rainfall event of July 4, 2020, was compared with the flood marks and water levels at several observatories. Then, rainfall–runoff discharge simulations with the SFM for the Ichifusa and Kumagawa dam catchments are carried out using the three rainfall ensemble forecasts as inputs. Finally, ensemble flood simulations with SWE were carried out using the discharges from the two dam catchments driven by the 1000 member (LETKF) ensemble forecasts.

2.3 Flood simulation conditions

Figure 5 shows the observed inflow and outflow of the Ichifusa dam. In the actual situation of 2020, the emergency spillway gate release operation was considered in the dam, but it was avoided in the end. The total storage volume of the dam is 40.2 million m³, and the effective volume is 35.1 million m³. On the other hand, Fig. 5 also shows the simulated inflow at Kawabegawa dam conducted by Sumi and Nohara (2020) using a kinematic wave-type distributed rainfall–runoff model. This value is used as the pseudo-observation in the following as it was simulated using a physically based runoff model. The model parameter by

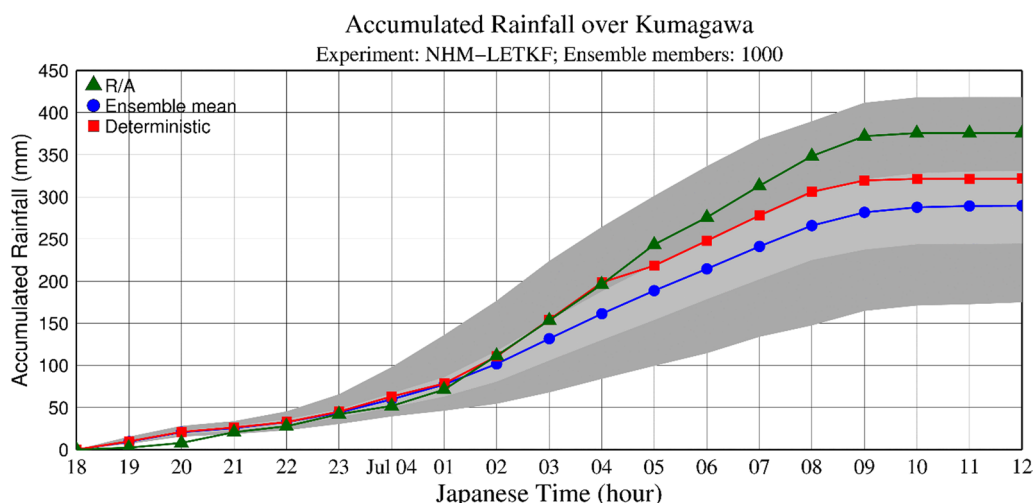


Fig. 3 Evolutions of the accumulated precipitation averaged over the Kumagawa catchment as forecasted by NHM-LETKF. The light gray zone represents the intervals between the first and third quartiles of the probability density functions of the accumulated rainfall. The dark gray zone indicates the 95% confidence intervals, i.e., the intervals between the 2.5 and 97.5 percentiles, of the probability density functions of the accumulated rainfall (Reproduced Duc et al. 2021)

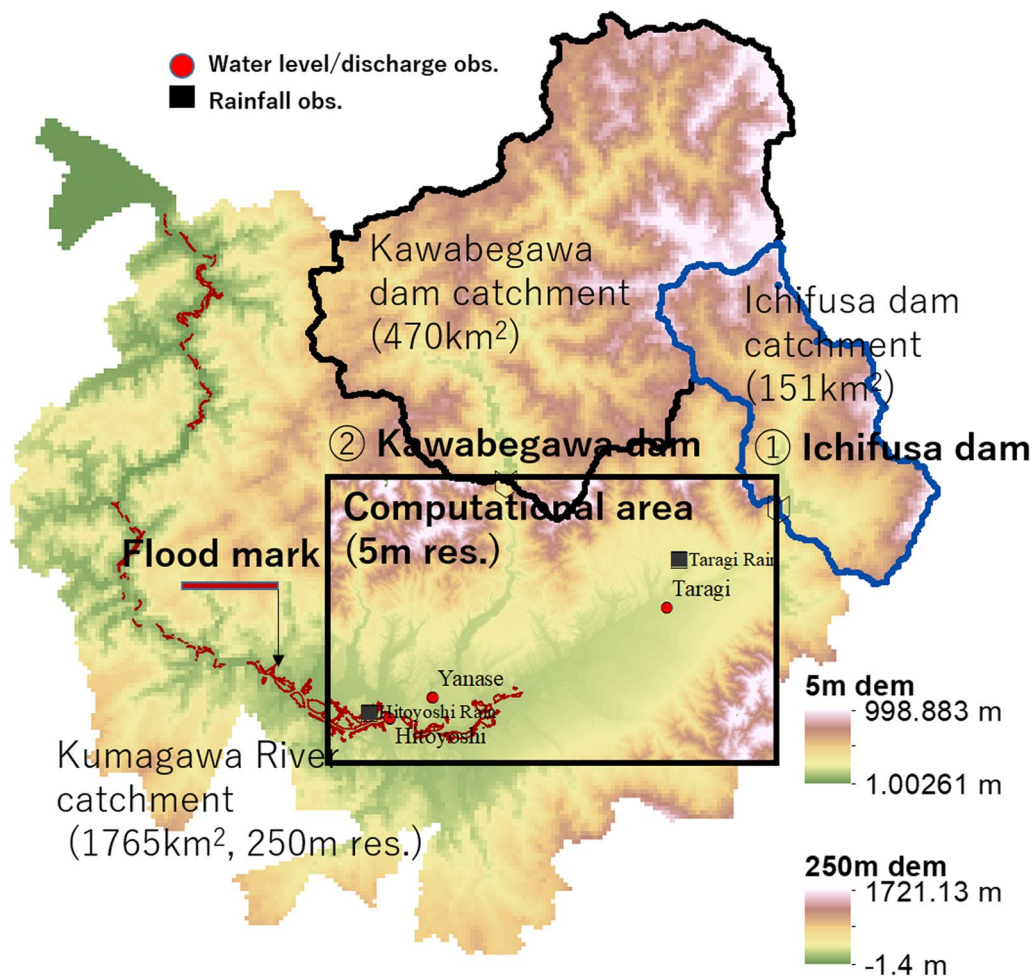


Fig. 4 Overview of the Kumagawa river catchment

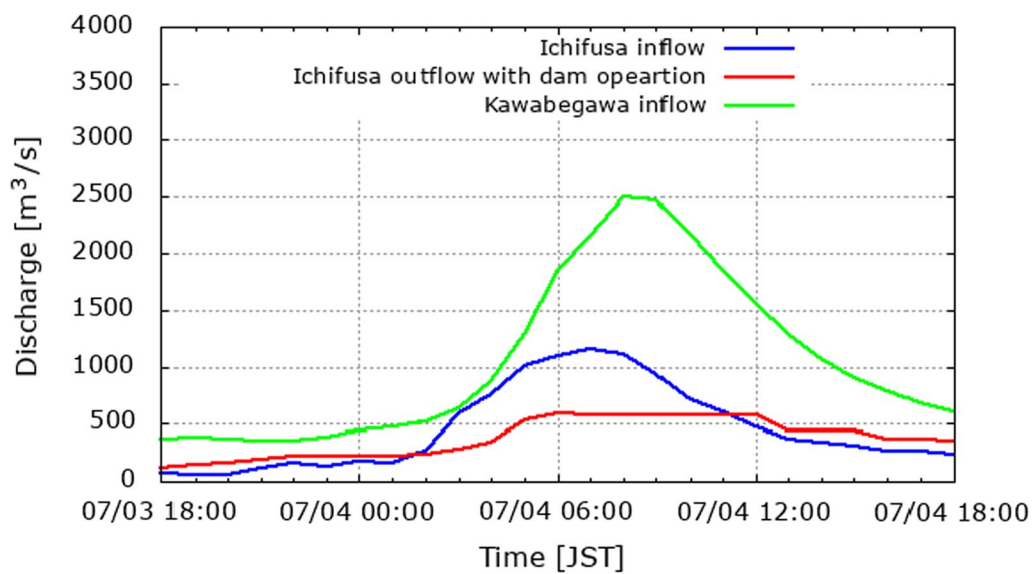


Fig. 5 Observed inflow/outflow of the Ichifusa dam and simulated inflow of assumed Kawabegawa dam by a distributed rainfall-runoff model (Sumi and Nohara 2020)

Sumi and Nohara (2020) was adjusted so that the simulated discharge was fitted to the observation at Yanase (Fig. 4) in the downstream of Kawabegawa dam.

The observed outflow to Ichifusa dam after dam control and simulated inflow at the assumed Kawabegawa dam was provided to the flood simulation with the SWE at points 1 and 2 as shown in Fig. 4. As explained, the R/A was also provided in the entire computational domain. The flow can go out from the square boundary of the computational domain based on the weir formula. The governing equations of SFM and SWE models applied are as follows. The explanation of the Kalman filter used afterward is also described.

2.3.1 SFM

The equations of the storage function model and Kalman filter applied are written by referring to JSCE (2002). For the details see JSCE (2002).

A storage function model by Hoshi and Yamaoka (1982) (also in JSCE 2002) which is a function made up of two terms was used.

$$s(t) = k_1 q^{p_1}(t) + k_2 \frac{d}{dt} q^{p_2}(t) \tag{1}$$

where q is the direct runoff in [mm/h], t the time in [h], k_1, k_2, p_1, p_2 the model parameters. SFM is a lumped model and driven by the basin-average rainfall of the Ichifusa dam and Kawabegawa dam catchments. The parameters identified are given in Table 2.

Then, the continuity equation of the storage height is:

$$\frac{ds(t)}{dt} = cr(t) - q(t) \tag{2}$$

where c is the runoff ratio and r is the catchment-average rainfall intensity in [mm/h].

Inserting Eq. (1) into (2) yields

$$k_2 \frac{d^2 q^{p_2}(t)}{dt^2} = -k_1 p_1 q^{p_1-1}(t) \frac{dq(t)}{dt} + cr(t) - q(t) \tag{3}$$

Equation (3) can be transformed into a system of ordinary differential equations (ODEs).

$$\frac{dx_1(t)}{dt} = x_2(t) \tag{4}$$

$$\begin{aligned} \frac{dx_2(t)}{dt} = & -\frac{k_1 p_1}{k_2 p_2} x_1(t)^{p_1/p_2-1} x_2(t) \\ & -\frac{1}{k_2} x_1(t)^{1/p_2} + \frac{c}{k_2} r(t) \end{aligned} \tag{5}$$

where $x_1 = q^{p_2}, x_2 = \frac{dq^{p_2}}{dt}$.

By linearizing this ODE system, an update or system equation is obtained for an extended Kalman filter besides an observation equation derived from the observed discharge and also linearized:

System Equation (6)
 $x(k+1) = \Phi(k)x(k) + \alpha(k) + u(k)$

Observation Equation (7)
 $y(k) = \Gamma(k)x(k) + \beta(k) + w(k)$

where the variables are denoted as follows: k : time. x : system state variable (p -dimensional vector). Φ : state transition matrix ($p \times p$ matrix). α : system constant vector (p -dimensional vector). u : system noise, independent normal Gaussian white noise with zero mean and U variance (p -dimensional vector). y : observation vector (m -dimensional vector ($m \leq p$)). Γ : observation matrix ($m \times p$ matrix). β : observation constant vector (m -dimensional vector). w : observation noise, independent normal Gaussian white noise with zero mean and W variance (p -dimensional vector).

The exact form of the two matrices $\Phi(k), \Gamma(k)$ and the two vectors $\alpha(k), \beta(k)$ is given in JSCE (2002). Referring to Eqs. 4 and 5, state variables of Eq. (6) to be estimated by the extend Kalman filter are defined as follows:

$$\begin{aligned} x_1 = q^{p_2}, x_2 = \frac{dq^{p_2}}{dt}, x_3 = k_1, x_4 = 1/k_2, \\ x_5 = p_1, x_6 = 1/p_2, x_7 = c \end{aligned} \tag{8}$$

The initial estimation of the seven state variables above must be given. Likewise, estimated error covariance matrix, the covariance matrix of the system noise and observation noise must be also initially given for the application. Then, the state variables are updated at each time step following the algorithms of the extended Kalman filter including the calculation of the Kalman gain. See JSCE (2002) for further details.

2.3.2 SWE

$$\frac{\partial h}{\partial t} + \frac{\partial M}{\partial x} + \frac{\partial N}{\partial y} = R \tag{9}$$

Table 2 Parameter values for SFC

| Parameters | k_1 | k_2 | p_1 | p_2 |
|------------|-------|-------|-------|-------|
| Ichifusa | 16.0 | 47.6 | 0.650 | 0.46 |
| Kwabegawa | 14.1 | 66.7 | 0.515 | 0.50 |

$$\frac{\partial M}{\partial t} + \frac{\partial uM}{\partial x} + \frac{\partial vM}{\partial y} = -gh \frac{\partial H}{\partial x} - gn^2 u \frac{\sqrt{u^2 + v^2}}{h^{1/3}} \tag{10}$$

$$\frac{\partial N}{\partial t} + \frac{\partial uN}{\partial x} + \frac{\partial vN}{\partial y} = -gh \frac{\partial H}{\partial y} - gn^2 v \frac{\sqrt{u^2 + v^2}}{h^{1/3}} \tag{11}$$

where h is the surface flow water depth; M , N the discharge fluxes in the x - and y -directions, respectively ($M=uh$, $N=vh$); R the rainfall intensity; u , v the surface flow velocities in the x - and y -directions, respectively; H the water level ($h+z$); n the Manning’s roughness coefficient; g the acceleration due to gravity. This SWE model was parallelized by MPI and Open MP (Kobayashi et al. 2016b). The computational area of the region is 26.545 km × 16.995 km with 5 m resolution; thus, the number of computational grids is 5309 × 3399 = 18,045,291. The initial time of the simulation was 18JST July 3, 2020, and the simulation was carried out for 24 h. The Manning’s roughness coefficient n in Eqs. (10–11) is 0.05.

Figure 6 shows the simulated water depth in the computational domain. The figure also shows the inundation area record by GSI at downstream. The right-hand figure is an enlarged view around Hitoyoshi city. Overall, it is clear that the simulated inundated area is in good agreement with the area where the record by GSI exists. The simulated water levels at Yanase, Hitoyoshi and Taragi water level observatories were compared with the observed water levels as shown in Fig. 7. Since there is no water in the beginning of the simulation, the difference in the beginning of the simulation is large but the levels at

the peaks were basically in good agreement for the prediction of the inundation level. The observation at Hitoyoshi was missing from the middle due to the flooding.

3 Results and discussion

3.1 Ensemble rainfall–runoff simulations at Ichifusa dam

As mentioned, SFM by Hoshi and Yamaoka (1982) was used for the simulation of dam inflow at Ichifusa and Kawabegawa dams. The reason to use this simple conceptual rainfall–runoff model is that the computational speed is fast. A 1000-member ensemble flood simulation with 1000 rainfalls and SFM needs approx.15 s. using a workstation with Xeon CPU E5-2670 (2.6 GHz).

In the followings, the comparisons with the 21-member ensemble by MEPS of JMA (hereafter 21 (MEPS)), the 100-member ensemble by 4D LETKF (hereafter 100 (LETKF)) and the 1000-member ensemble by 4D LETKF (hereafter 1000 (LETKF)) are carried out. Likewise, ten 100-member ensembles selected from 1000 (LETKF) are also compared. These ten 100-member ensembles are simply selected as members 1–100, 101–200, 201–300, ..., 900–1000 (hereafter expressed such as m1-100, m900-1000).

Figure 8a–c shows the catchment-average rainfalls of the Ichifusa dam basin with 21(MEPS), 100 (LETKF) and 1000 (LETKF), respectively. Both of 100 (LETKF) and 1000 (LETKF) started at 18:00 on July 3 for 24 h, while 21 (MEPS) started at 21:00 on July 3 for 39 h. The figures show that the ensemble means of the 21 and 100 members clearly underestimate R/A which is in the paper regarded as the observed rainfall. Likewise, the gray clouds of ensembles by 21 and 100 ensemble members

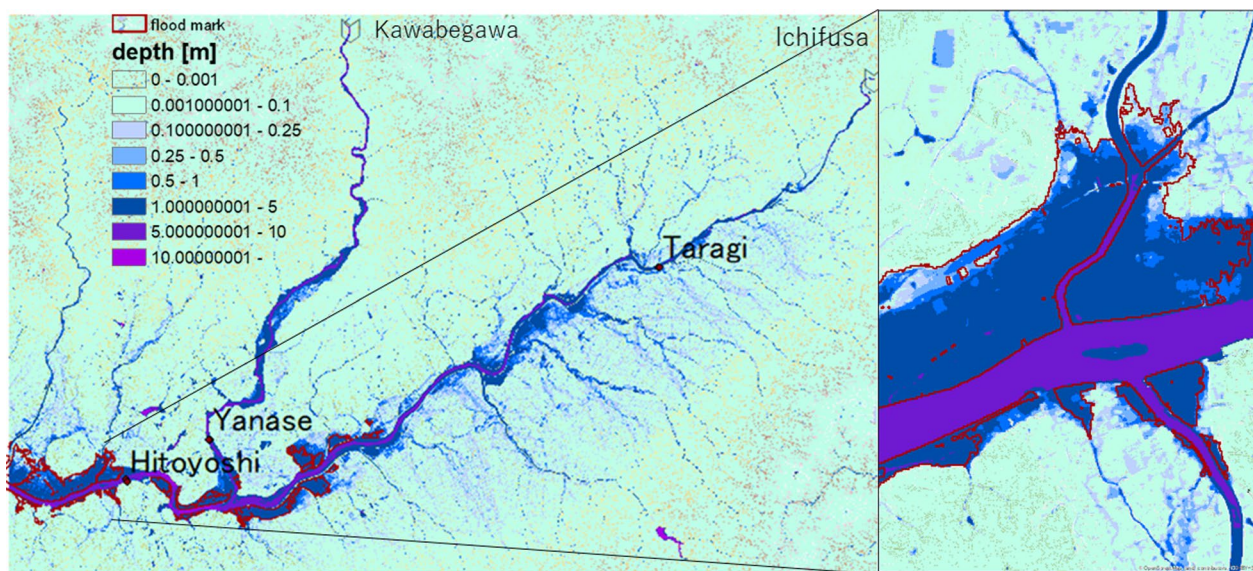


Fig. 6 Simulated water depth (2020/7/4, 0900)

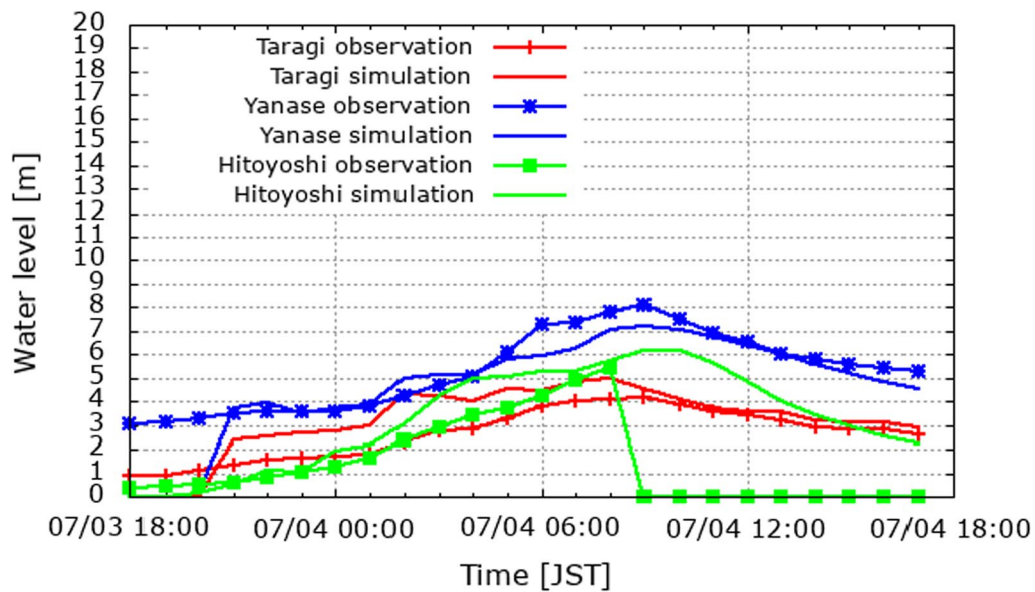


Fig. 7 Observed and simulated water depth at water level observatories

can not necessarily cover the peak of R/A, while those by 1000 members cover the entire R/A except the very beginning of the rainfall. Figure 8d–f shows the cumulative rainfall. The mean of the 1000-member ensemble shows good agreement with that by R/A. Likewise, the mean of the 100 ensemble rainfalls shows a relatively good agreement with R/A although it is a little underestimation. The mean of the 21-member ensemble clearly underestimates R/A.

Figure 9a–c shows the simulated 21 (MEPS), 100 (LETKF) and 1000 (LETKF) ensemble discharges by SFM. Same as rainfall, the gray cloud of 1000 member discharges covers the observation, while that by 21 members could not encompass the observation though 1 out of 21 members having maximum peak discharges shows a good agreement with the observation. Several members in the 100-member ensemble prediction also show a relatively good agreement with the observation, though the peaks of many members appear earlier than the observation and the peak discharges are underestimated. The ensemble mean of 1000 members relatively resembles the observation, while those of 21 and 100 members clearly underestimate the observation. Figure 9d–f shows cumulative discharges. The mean of 1000 members shows a good agreement with the observation, though it is slightly underestimated. On the other hand, the final value of the mean of 100 members also shows a good agreement with the observation. The mean of 21 members underestimates the observation largely. Good prediction of cumulative inflow volume is also useful for reservoir managers

to know if the flood control capacity of the reservoir is much enough.

3.2 Selective 100-member ensembles from the 1000-member weather and rainfall–runoff simulation at Ichifusa dam

Figure 10a shows again 1000 (LETKF) ensemble discharge simulations, while figure b–f shows the 100-member ensembles selected from 1000 members. The members are denoted by m1-100, m101-200, ..., m401-500. From the visual judgment only, each of the 100 selected members shows similar results. To quantify the agreement with the observation, Nash–Sutcliffe efficiency (hereinafter NSE: Nash and Sutcliffe 1970) is calculated.

$$NSE = 1 - \frac{\sum_{i=1}^N \{Q_0^i - Q_s^i\}^2}{\sum_{i=1}^N \{Q_0^i - Q_m\}^2} \tag{12}$$

$$Q_m = \frac{1}{N} \sum_{i=1}^N Q_0^i \tag{13}$$

where N is the total number of time steps (1 h interval), Q_0^i is the observed dam inflow (discharge) at time i , Q_s^i is the simulated dam inflow (discharge) at time i , Q_m is the average of the observed dam inflows.

NSEs are shown in Fig. 11. Figure 11a, c shows all the NSEs of 21 (MEPS), 100 (LETKF), 1000 (LETKF) and 10 selected 100-member ensembles from 1000 (LETKF) with regard to rainfall and discharge, respectively.

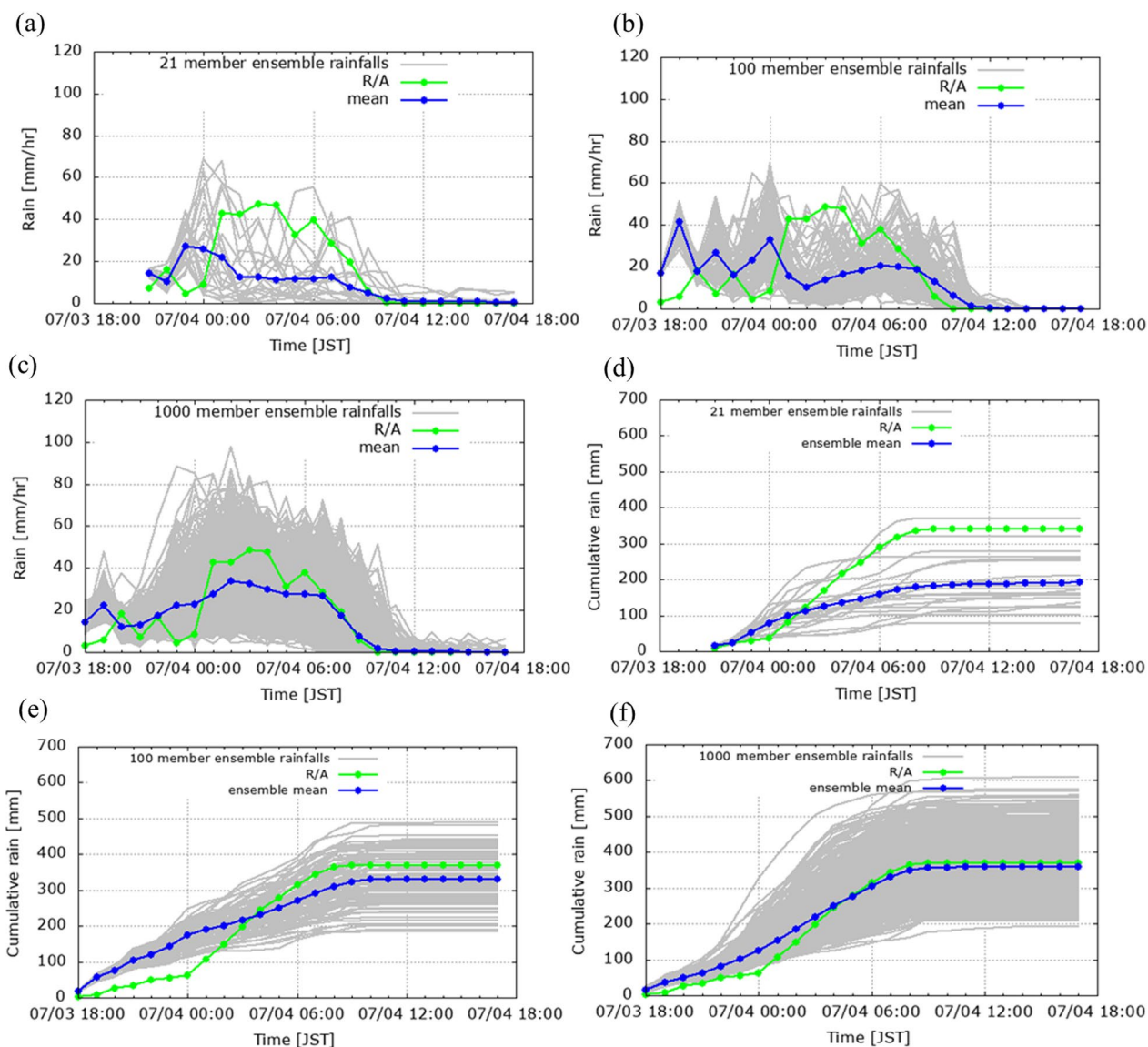


Fig. 8 Observed and simulated basin-average rainfalls for Ichifusa dam catchment. **a–c** Hourly rainfall intensity of **(a)** 21 members (MEPS), **(b)** 100 members (LETKF) and **(c)** 1000 members (LETKF) **d–f** Cumulative rainfall for **(d)** 21 members (MEPS), **(e)** 100 members (LETKF) and **(f)** 1000 members (LETKF)

Figure 11b, d shows the box plot of the NSEs also for rainfall and discharge, respectively. From these figures, 1000 (LETKF) clearly outperforms 100 (LETKF) and 21 (LETKF) for both rainfall and discharge. However, it is recognized that some NSEs of 21 (MEPS) and 100 (LETKF) are close to one, thus those members are in good agreement with the observations. On the other hand, each of the selected 100-member ensembles shows a similar tendency with 1000 (LETKF). In other words, each of the 100-member ensembles is randomly selected so that the set has similar statistics to the 1000-member ensemble. Note that even though the number of members is the same in the both 100

(LETKF) and 100 (selective) cases, the two sets are not equal in the sense that the selective 100-member ensembles inherit all statistics from the larger 1000-member ensemble, and therefore should be understood as representatives of this large ensemble. A large number of ensemble members enable us to better capture uncertainties in atmospheric processes, and to better utilize information provided by observations, thus leading to significant improvement in rainfall forecast. These 10×100 member sets also outperform 21 (MEPS) and 100 (LETKF) for both rainfall and discharge.

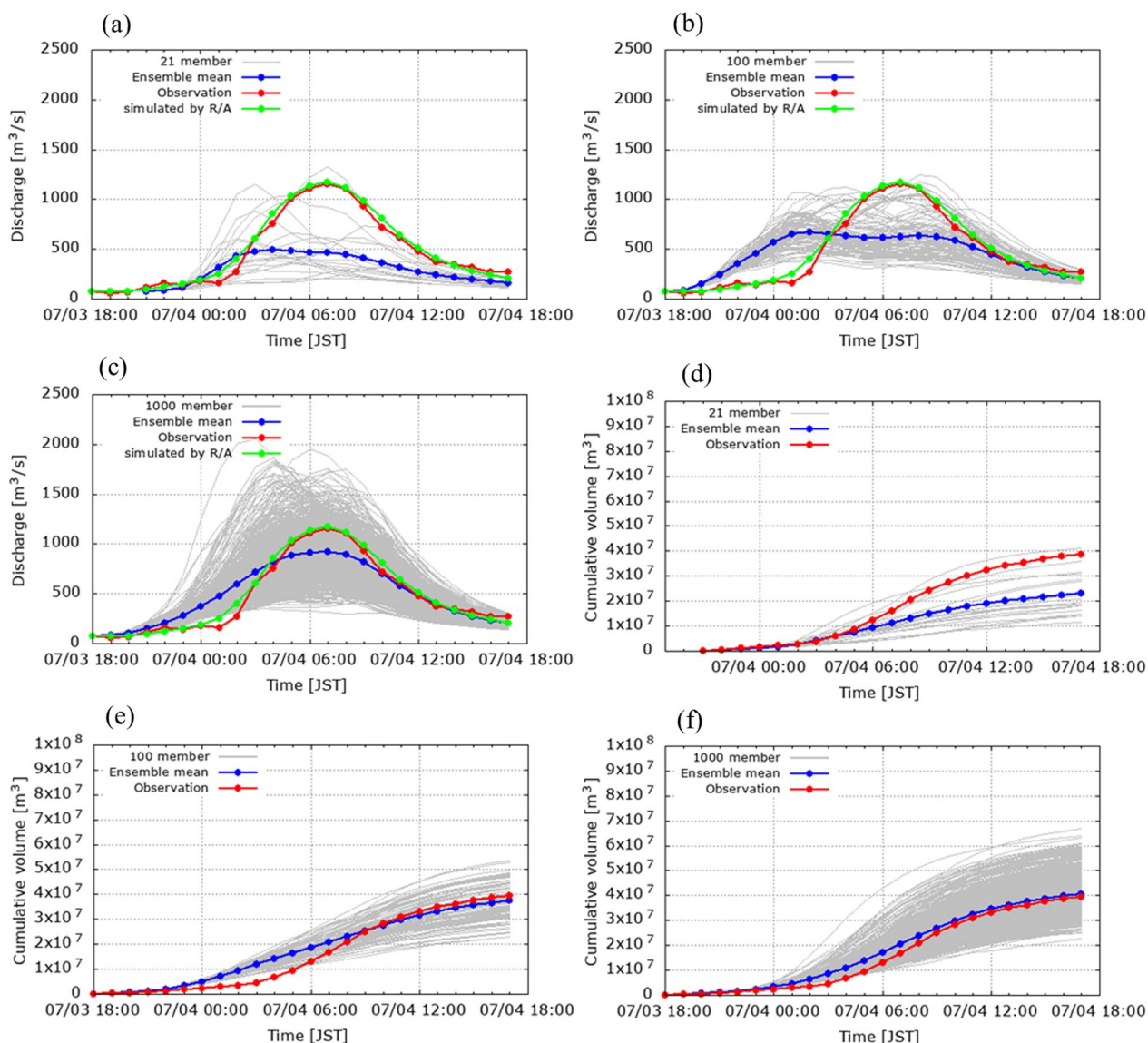


Fig. 9 Observed and simulated discharge to Ichifusa dam catchment. **a–c** Hourly discharge of (a) 21 members (MEPS), (b) 100 members (LETKF) and (c) 1000 members (LETKF). **d–f** Cumulative discharge for (d) 21 members (MEPS), (e) 100 members (LETKF) and (f) 1000 members (LETKF)

3.3 Ensemble rainfall–runoff simulations at the assumed Kawabegawa dam

Figure 12a–c shows the ensemble basin-average rainfalls for the Kawabegawa dam catchment. Again, each member of the 21-member (MEPS) ensemble and its mean clearly underestimate R/A. Those 100 (LETKF) members are better than the 21 members in terms of the amount, though the cloud of 100 members could not partially cover R/A. The cloud of 1000 (LETKF) members entirely covers R/A well, though the mean still underestimates R/A. Figure 12d–f shows the cumulative rainfalls. The cumulative rainfall of 1000 (LETKF) members resembles that of R/A very well. That of 100 (LETKF) members also

shows a relatively good agreement with R/A while that of 21 (MEPS) members clearly underestimates R/A.

Figure 13a–c shows the simulated discharges by SFC for 21 (MEPS), 100 (LETKF) and 1000 (LETKF) members. The 21 member discharges clearly underestimate the discharge observation. On the other hand, the clouds of 100 and 1000 members cover the observation well. It should be noted that the 100-member ensemble also shows good results with regard to the Kawabegawa dam catchment. Some members of the 100-member ensemble show a good agreement with the observation. Likewise, the 1000-member ensemble well covers the observation. Considerable members of the 1000-member ensemble

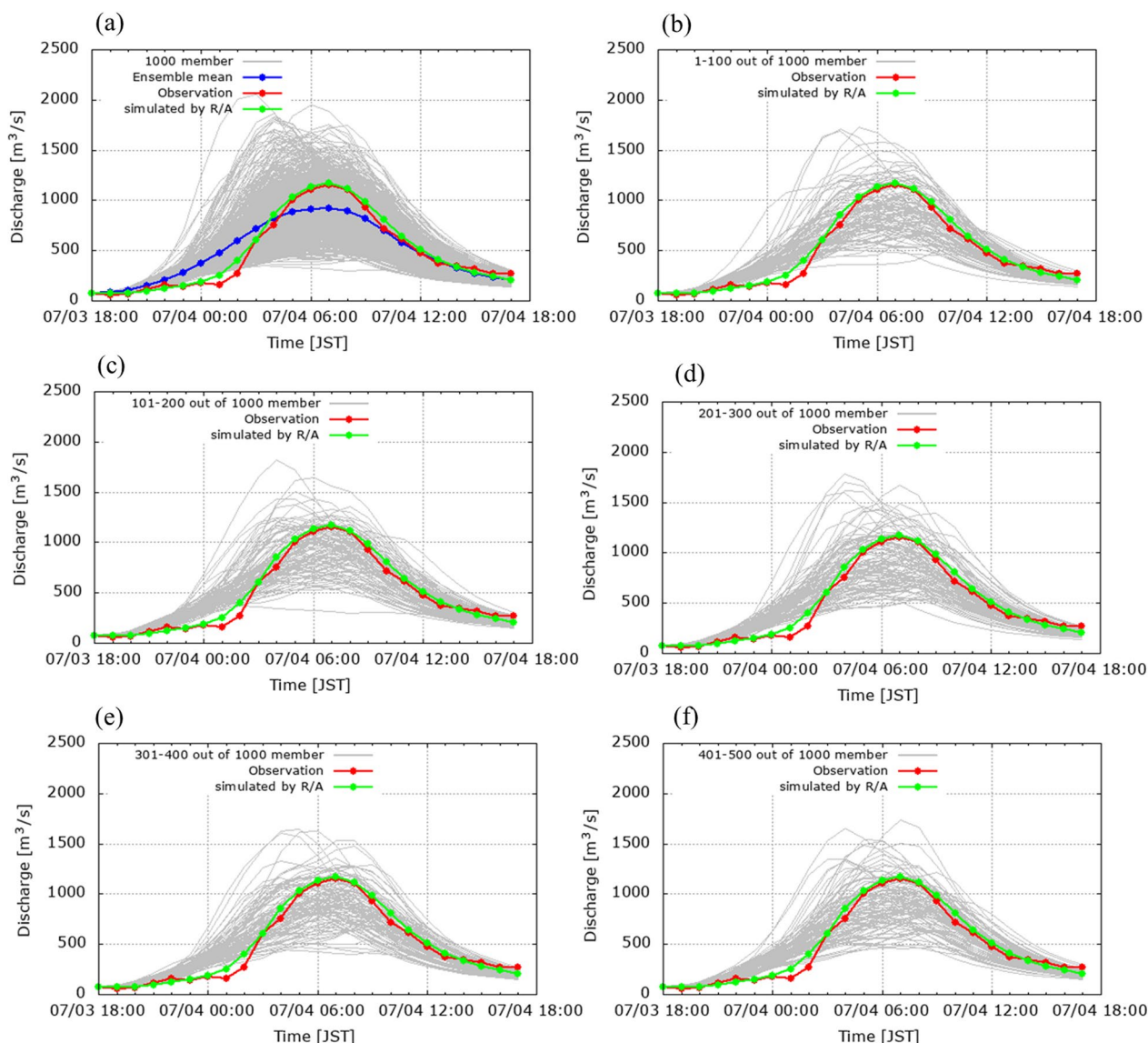


Fig. 10 Observed and simulated discharge to Ichifusa dam catchment by 1000 (LETKF). **a** Hourly discharge of 1000 members, **b** of m1-100, **c** m101-200, **d** m201-300, **e** m301-400, **f** m401-500

show a good agreement with the observation. The means of both 100 (LETKF) and 1000 (LETKF) members show good agreement with the observation.

3.4 Selective 100-member ensembles from the 1000-member ensemble weather and rainfall-runoff simulations at Kawabegawa dam

Figure 14a shows again 1000 (LETKF) ensemble discharge simulations for Kawabegawa dam, while Fig. 14b–f shows the 100-member ensembles selected from the 1000-member ensemble. Same as Ichifusa, the members are denoted by m1-100, m101-200,...

m401-500. Each of the selected 100-member ensembles shows similar results as the case of Ichifusa.

NSEs for Kawabegawa dam are shown in Fig. 15. Figure 15a, c shows all the NSEs of 21 (MEPS), 100 (LETKF), 1000 (LETKF) and 10 selected 100-member ensembles from 1000 (LETKF) for rainfall and discharge, respectively. Figure 15b, d shows the box plots also for the rainfall and discharge, respectively. From these figures, 1000 (LETKF) clearly outperforms 100 (LETKF) and 21 (LETKF) for rainfall. On the other hand, with regard to discharge, 100 (LETKF) shows an equivalent level of accuracy with 1000 (LETKF). Likewise, it is recognized that some NSEs of 21 (MEPS) and a considerable number

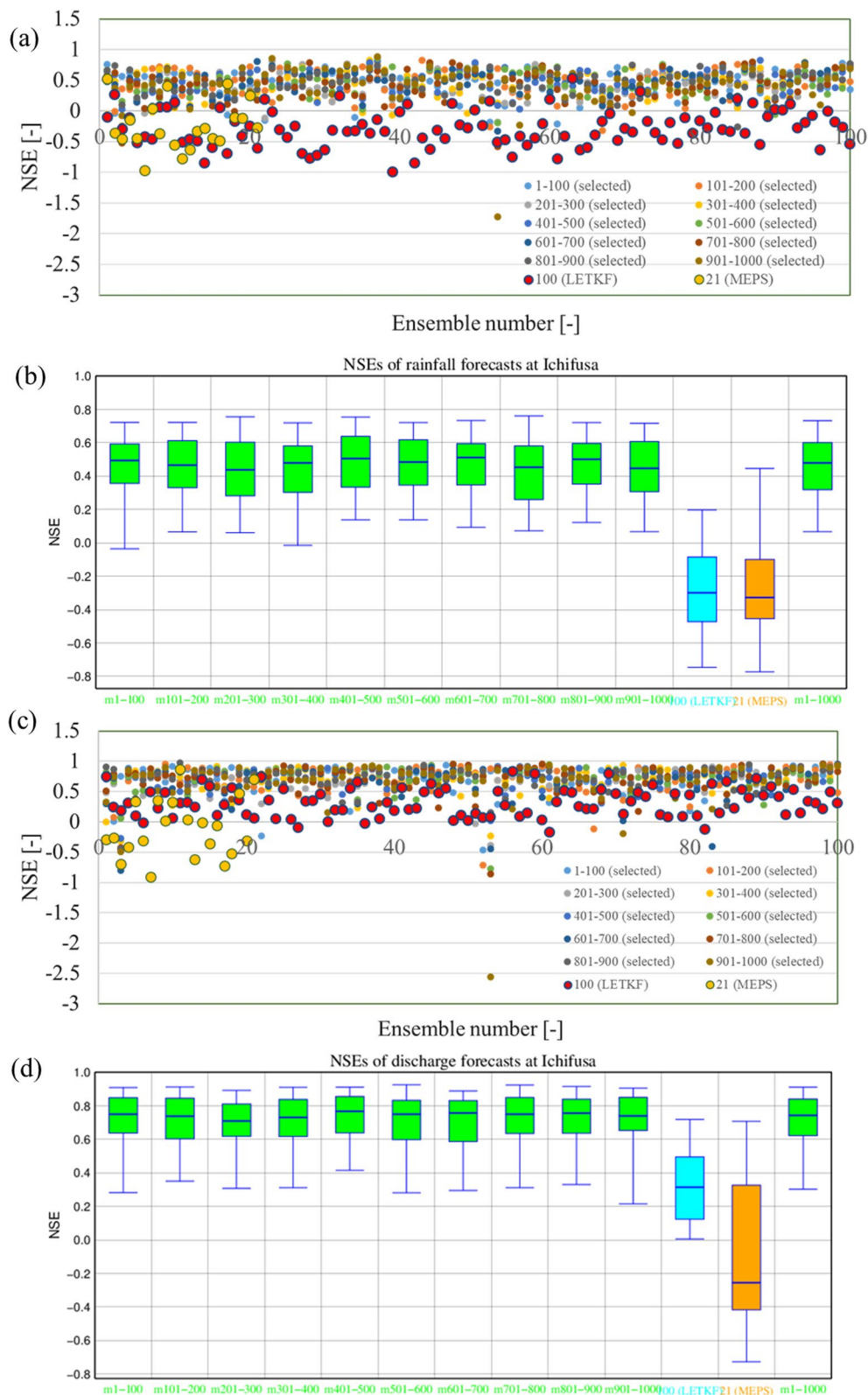


Fig. 11 a NSEs of rainfall, b NSE box plots of rainfall, c NSEs of discharge and d NSE box plots of discharge for Ichifusa dam

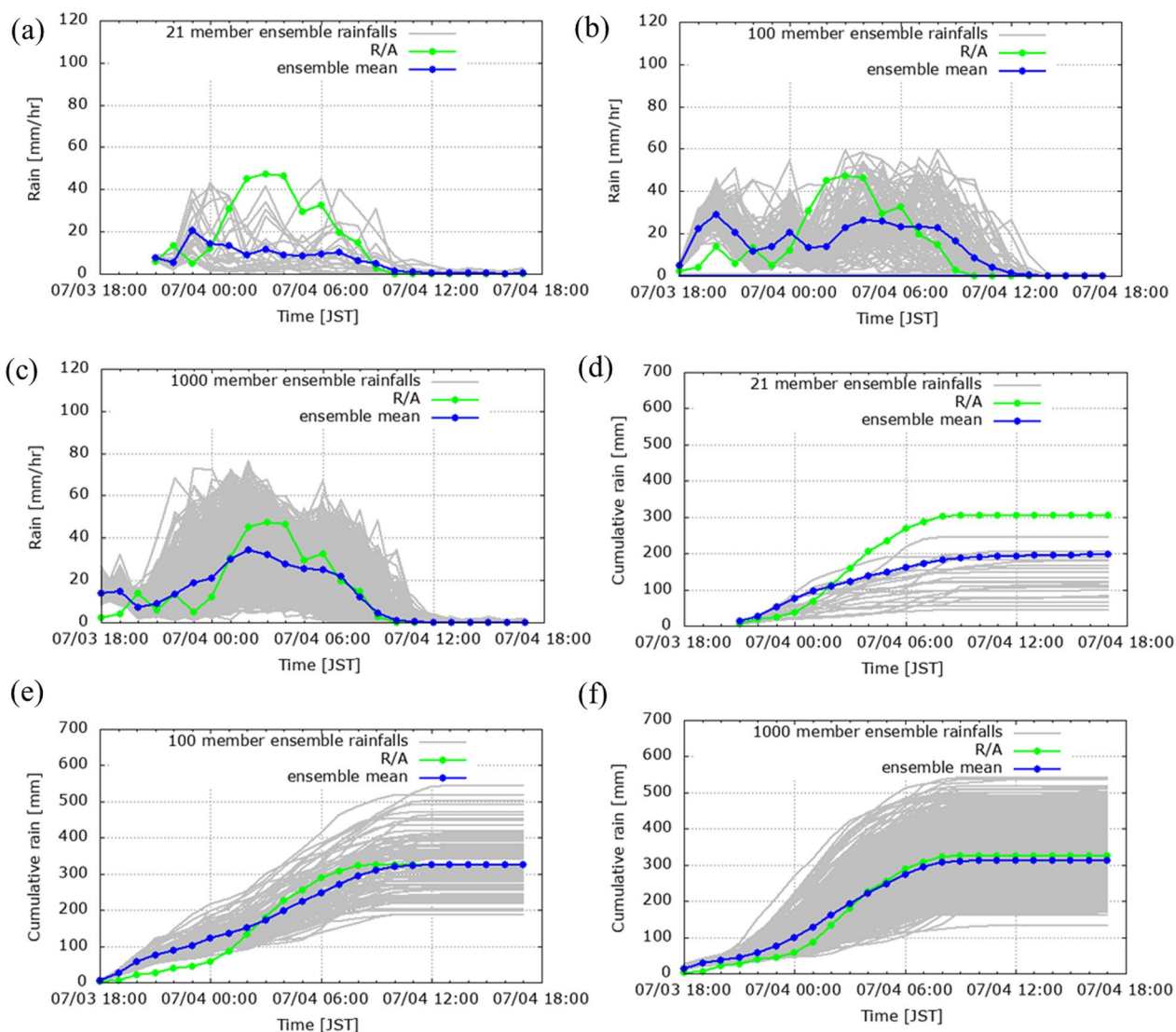


Fig. 12 Observed and simulated basin-average rainfalls for Kawabegawa dam catchment. **a–c** Hourly rainfall intensity of **(a)** 21 members (MEPS), **(b)** 100 members (LETKF) and **(c)** 1000 members (LETKF) **d–f** Cumulative rainfall for **(d)** 21 members (MEPS), **(e)** 100 members (LETKF) and **(f)** 1000 members (LETKF)

of 100 (LETKF) are close to one, or in good agreement with the observations. On the other hand, each of the selected 100-member ensembles shows a similar level of accuracy with 1000 (LETKF) and resembles them in statistics.

3.5 Ensemble flood simulation with a shallow water model

Then, ensemble inundation simulations are carried out using 1000 (LETKF) ensemble discharges at Ichifusa/Kawabegwa dams and the corresponding ensemble rainfalls in the previous chapters as inputs. The results are shown in Fig. 16. The figure shows the probabilities of the maximum inundation depth of the selected ensemble members beyond the maximum inundation depth simulated by

R/A without the discharge cut of dams as shown on the right-hand side. Herein, 1–100, 1–200, 1–500 and 1–1000 members are selected. As in the figures, the probability becomes even more than 50% in the mountain area whose maximum inundation depth is directly simulated by the ensemble rainfalls. However, in the main channels of the Kumagawa and Kawabegawa rivers, the probability is below 50%. One of the interesting features is that, as the case of discharges at the two dams in the previous chapters, the distribution of the probability does not differ much according to the number of selected ensembles. This may indicate that the place of inundation is governed mostly by the topography or ground elevation in addition to the rainfall distribution, thus the place where the

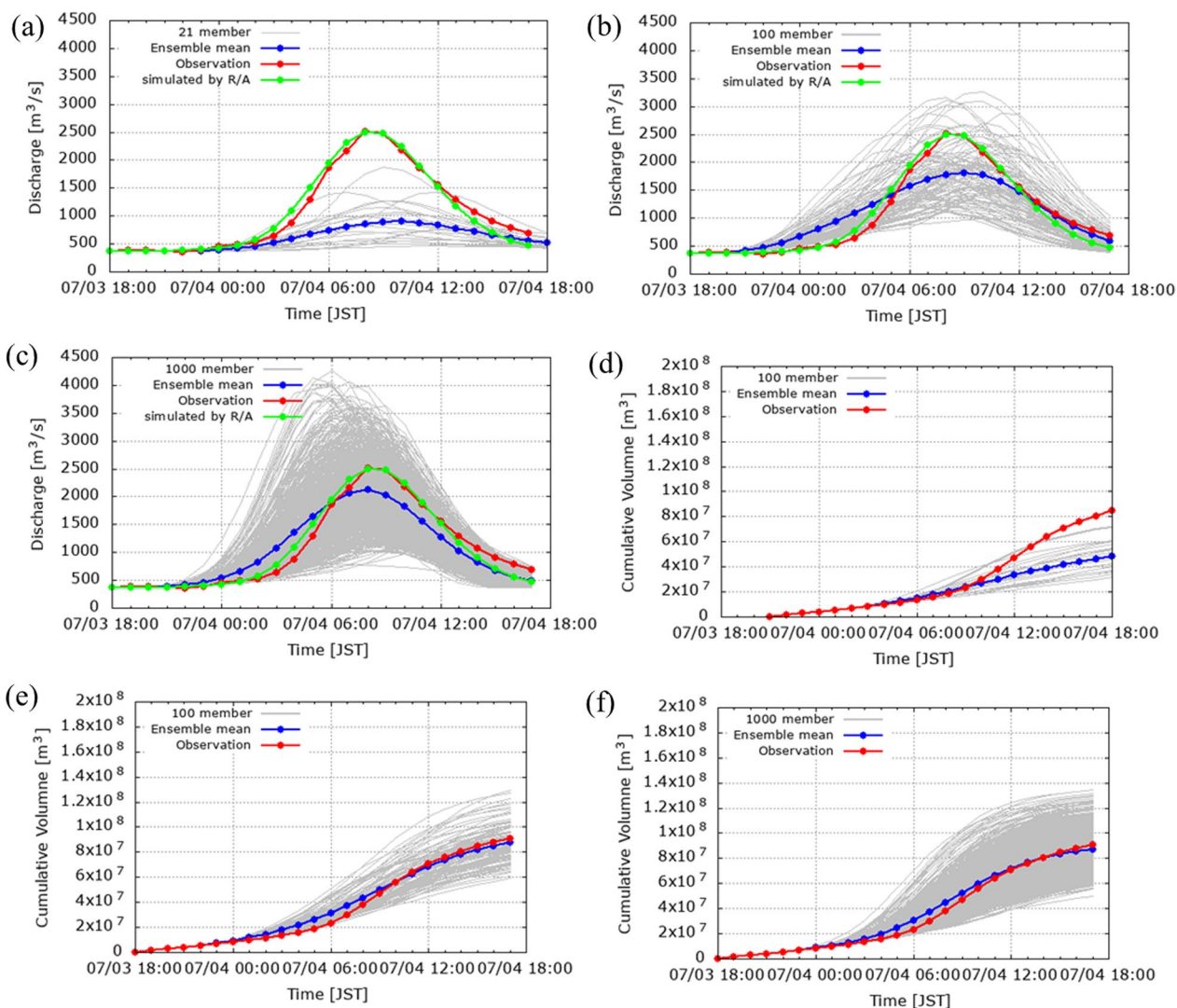


Fig. 13 Observed and simulated discharge to Kawabegawa dam catchment. **a–c** Hourly discharge of (a) 21 members (MEPS), (b) 100 members (LETKF) and (c) 1000 members (LETKF). **d–f** Cumulative discharge for (d) 21 members MEPS, (e) 100 members and (f) 1000 members

maximum inundation occurs does not differ much as the flood water flows into the lower elevation area. In other words, a reasonable number of ensemble members could be smaller when the inundation depth is predicted, unlike the three-dimensional weather ensembles.

3.6 Kalman filter application on the rainfall–runoff simulation

Finally, a Kalman filter (Kawamura 1993; JSCE 2002, Ueda 1984; Athans 1968) was applied to the first 11, 12, 13, 14, 15 and 16 h of the SFC ensemble simulations. Herein 21 (MEPS), 100 (LETKF) or 1000 (LETKF) state variable sets of SFC were adjusted so that simulated

hydrographs become similar to the observed discharge while the Kalman filter was applied. By doing this, the 21, 100 or 1000 simulated hydrographs become similar to the observation for the first 11–17 h, then the hydrographs afterward show the spread of the discharges according to the variations of ensemble rainfalls. This attempt was carried out since there are uncertainties in the runoff model state variables even against quasi-perfect rainfall (i.e., R/A). Thus, those uncertainties are minimized against the 1000 (LETKF) rainfalls. Note that the predicted rainfalls and not the observed rainfall are used in the Kalman filter. The challenge herein is to make a successful prediction beyond the accuracy of the rainfall predictions.

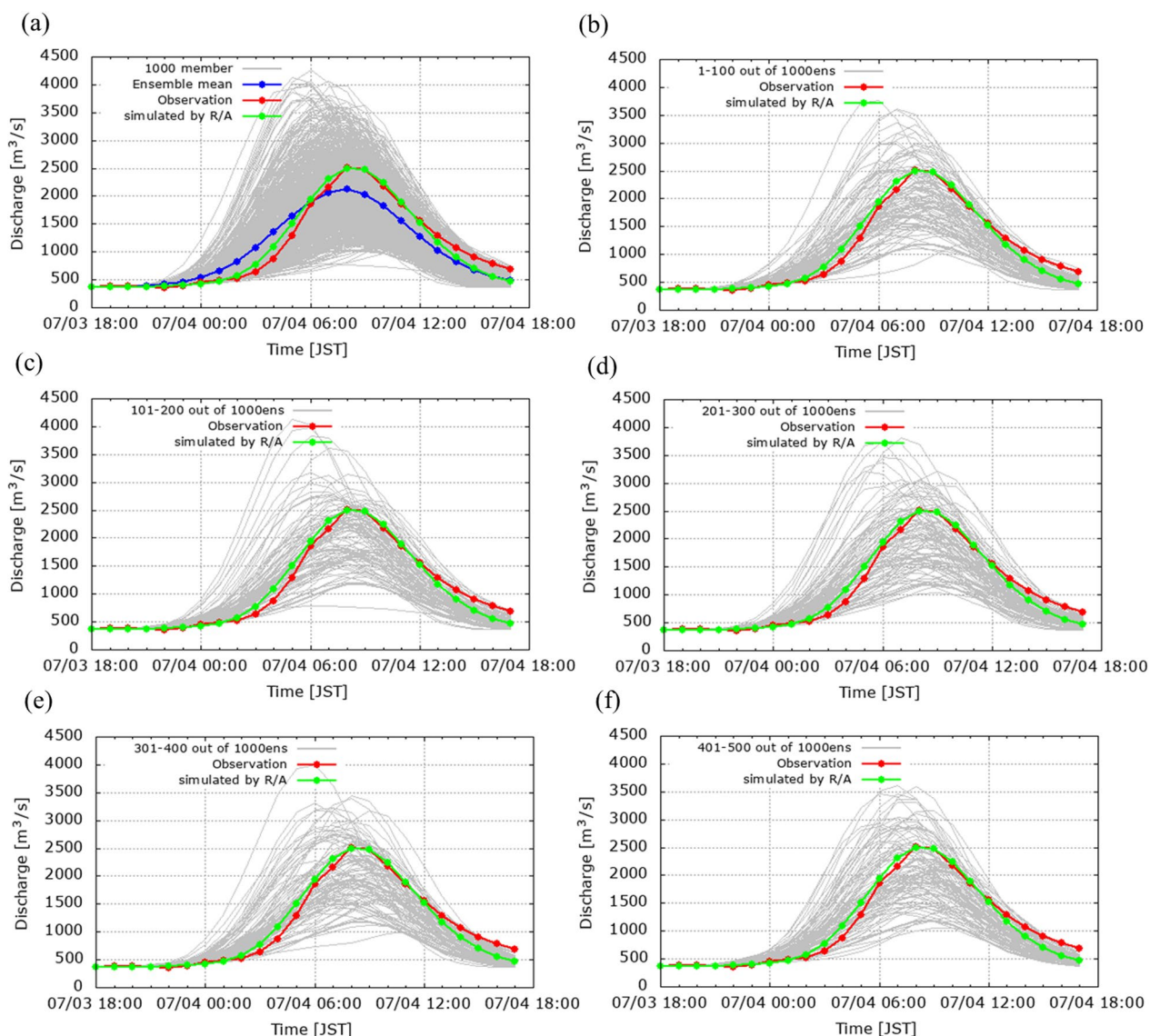


Fig. 14 Observed and simulated discharge to Kawabegawa dam catchment by 1000 (LETKF) **a** Hourly discharge of 1000 member, **b** of m1-100, **c** m101-200, **d** m201-300, **e** m301-400, **f** m401-500

Figure 17 shows the application of the Kalman filter on the discharge simulations of 21 (MEPS), 100 (LETKF) and 1000 (LETKF) ensembles for the Ichifusa dam. One of the interesting features of this Kalman filter application is that the ensemble mean becomes quite close to the observation especially as it approaches the peak discharge. The difference between the ensemble mean and observation is smaller in the case of the 1000 (LETKF)-member ensemble than the 21 (MEPS) or 100 (LETKF)-member ensembles with regard to Ichifusa dam. This indicates that 1000 ensemble simulations are superior to

100 or 21 ensemble simulations in this aspect because of fewer sampling errors. However, 1 of 21 ensemble members shows always a good agreement with the observation in this case which is preferable for the application of MEPS currently operated by JMA.

On the other hand, Fig. 18 shows the 21 (MEPS), 100 (LETKF) and 1000 (LETKF)-member ensembles for the Kawabegawa dam. In this case, the mean and ensembles of 21 members basically underestimate the observation. However, those of 100 and 1000 members show both good agreements. Although there are less large discharge

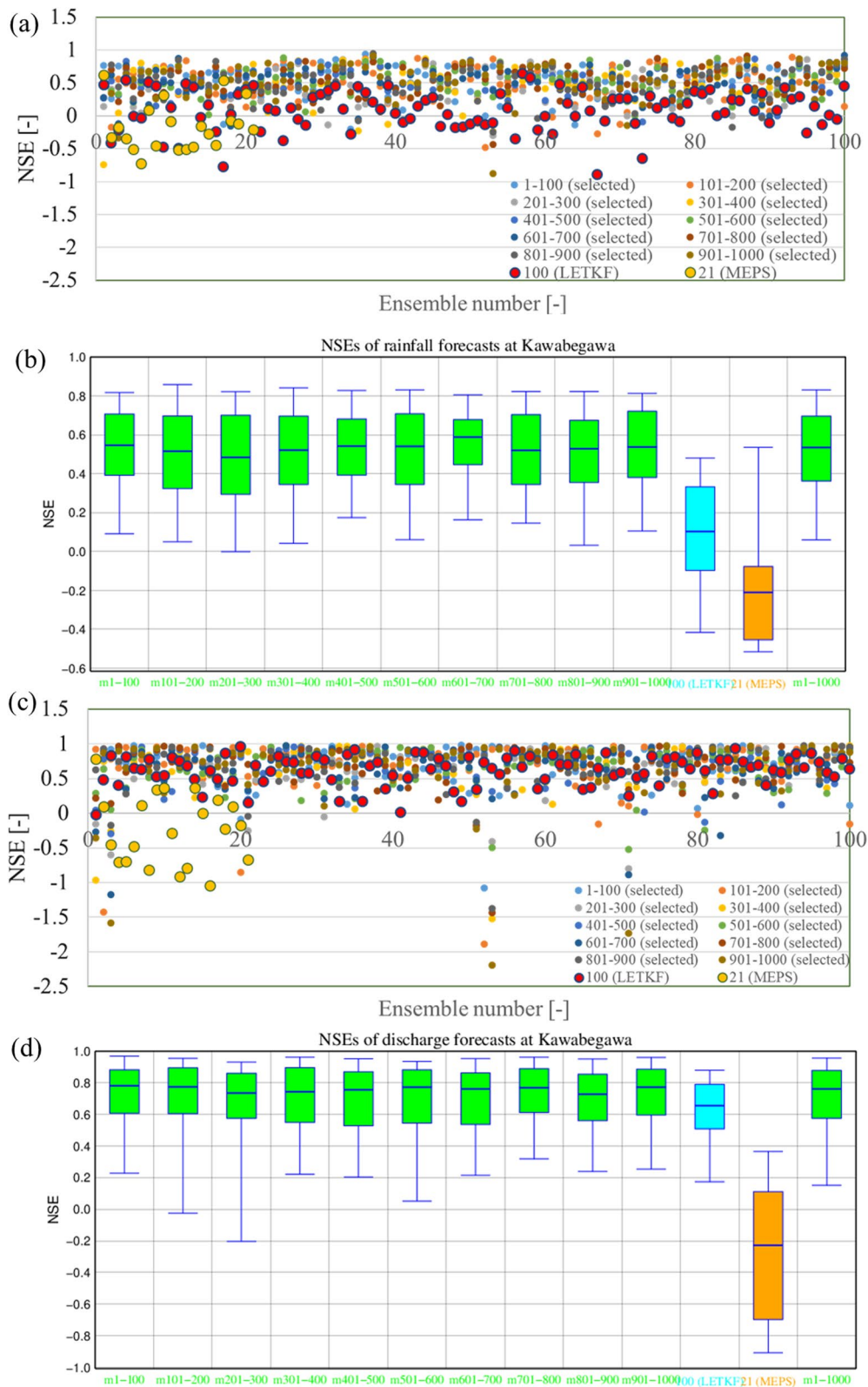


Fig. 15 a NSEs of rainfall, b NSE box plots of rainfall, c NSEs of discharge and d NSE box plots of discharge for Ichifusa dam

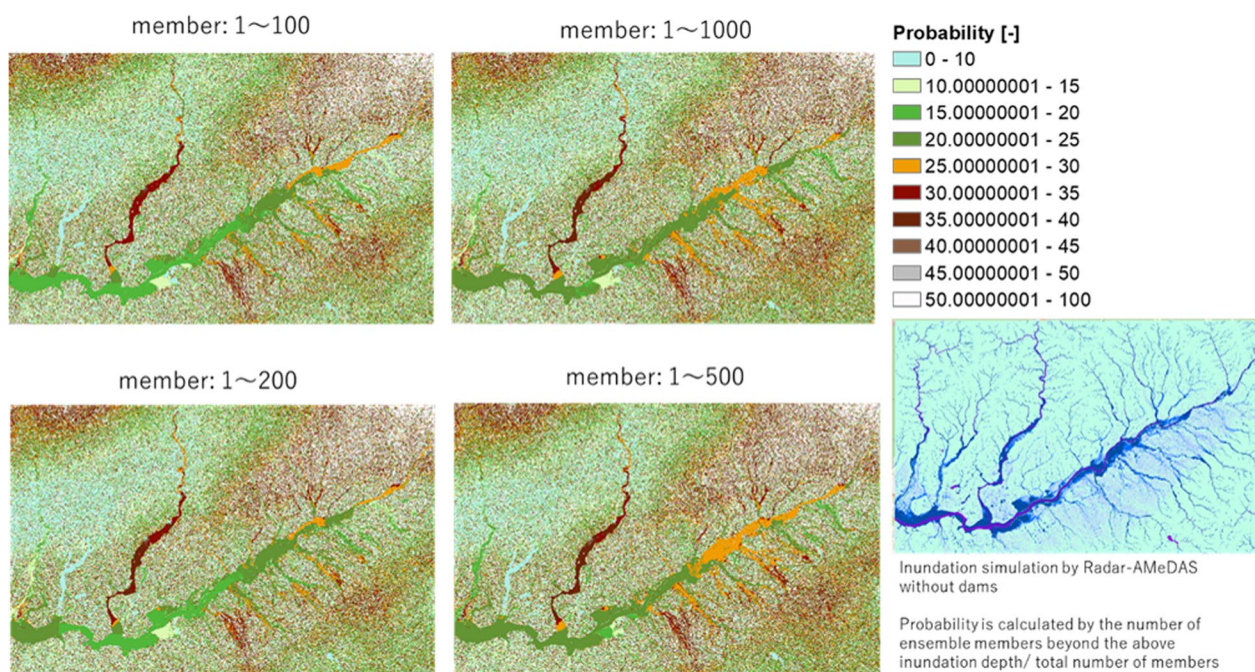


Fig. 16 The probabilities (%) of selected ensemble members beyond the inundation depth simulated by R/A

members in the 100-member ensemble compared with the 1000-member ensemble, the accuracy of the mean of 100 members compared with the observed discharge is not inferior to the 1000 members.

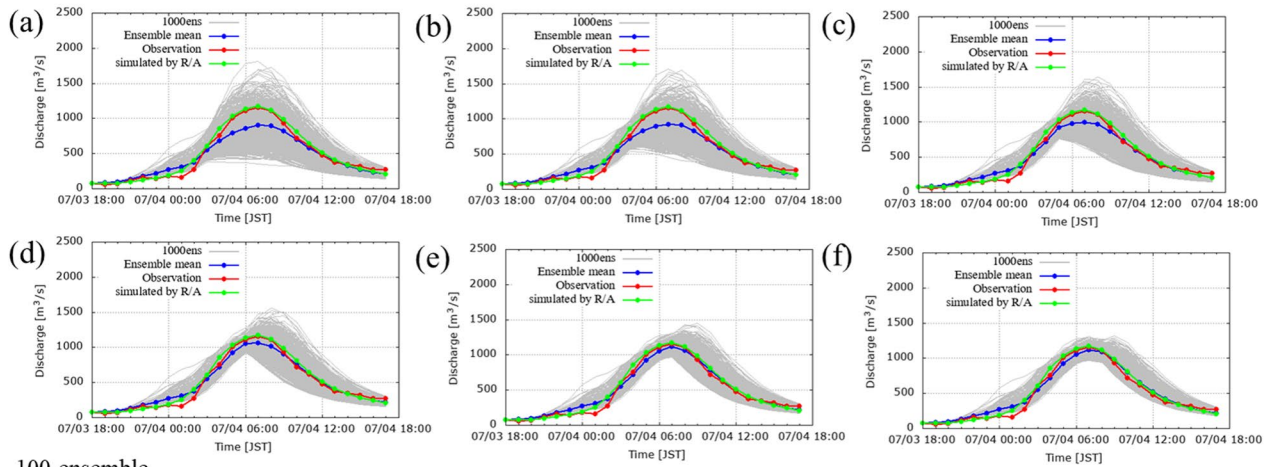
4 Conclusions

This paper dealt with the 1000 ensemble rainfall–runoff and inundation simulations driven by 1000 ensemble weather simulations. To better sample uncertainties in ensemble weather simulations, it is now prevailing to increase the number of ensembles even up to 1000–10,000 in the academic field of meteorology. Receiving these ensemble weather simulations, this paper carried out ensemble rainfall–runoff and inundation simulations. The results of discharge simulations at the Ichifusa and Kawabegawa dams using ensembles show that the overall trend of the rainfall–runoff simulation is similar to the weather simulation. In other words, the 1000 ensemble discharge simulations show basically better coverage of observed discharge as the case of ensemble rainfalls. Likewise, the ensemble mean of 1000 discharge simulations becomes closer to the observation, which is considered due to better representation in rainfall simulations.

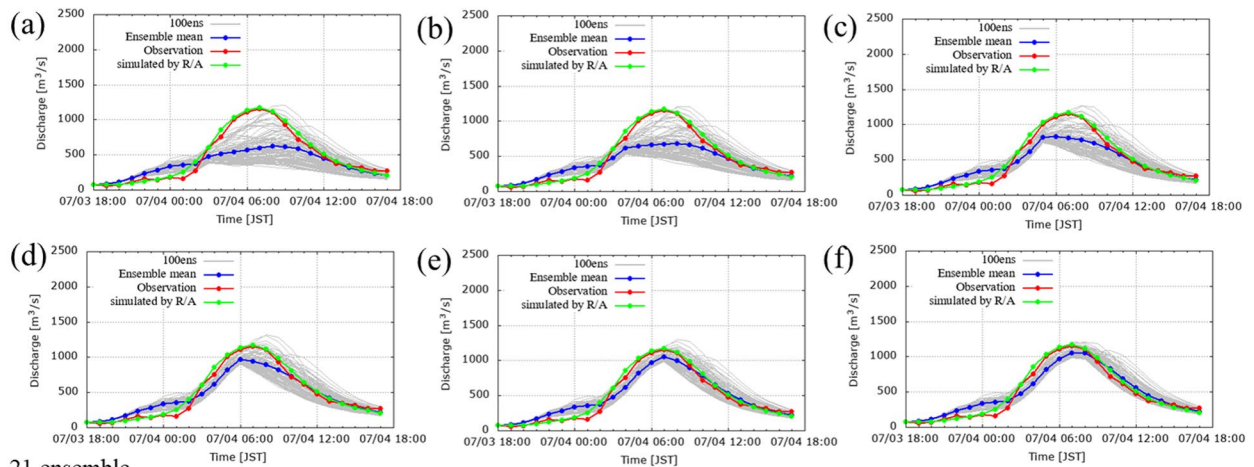
However, there were cases in the discharge simulation that the 100 (LETKF)-member ensemble was also

not bad. This is considered because the discharge by the rainfall–runoff simulation is determined not only by the rainfall but also by the topography and subsurface characters. The rainwater converged to the catchment outlet in case of rainfall–runoff simulation; thus, some differences of the rainfall pattern in the catchment could be canceled out. This means that the accuracy of discharge simulation is not necessarily the same to the accuracy of weather simulation if the soil parameter is appropriately set up. This change of accuracy is more confirmed when the state variables of the rainfall–runoff model are adjusted by the Kalman filter in real time using observations. If the real-time discharge observation exists 1–3 h ahead of the peak, the discharge prediction around peak time can be better. Nevertheless, 1000 ensemble simulations are preferable when the prediction long time before such as half to one day is necessary since the adjustment of rainfall–runoff model state variables has almost no meaning at the early stage when the rainfall prediction indicates small values. In this sense, the research on mega ensemble rainfall simulations with enough lead time is worth pursuing aiming at citizens an early evacuation before the flood incident occurs. Likewise, when 1000 ensemble inundation simulations were conducted, the results also indicated that the area where the maximum inundation occurs was determined again not only by the rainfall but also by the topography. Thus, the probability distribution of

1000 ensemble



100 ensemble



21 ensemble

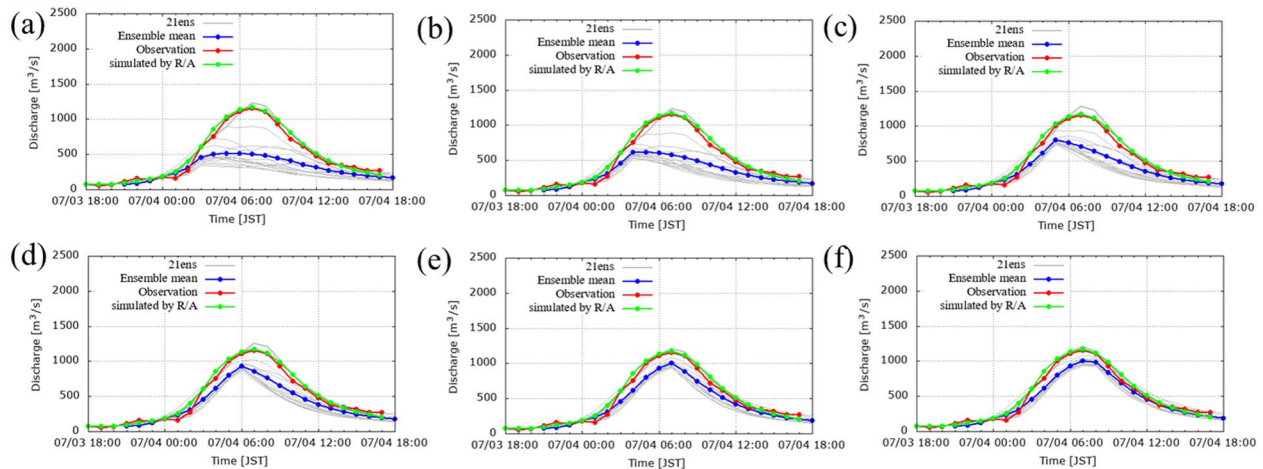
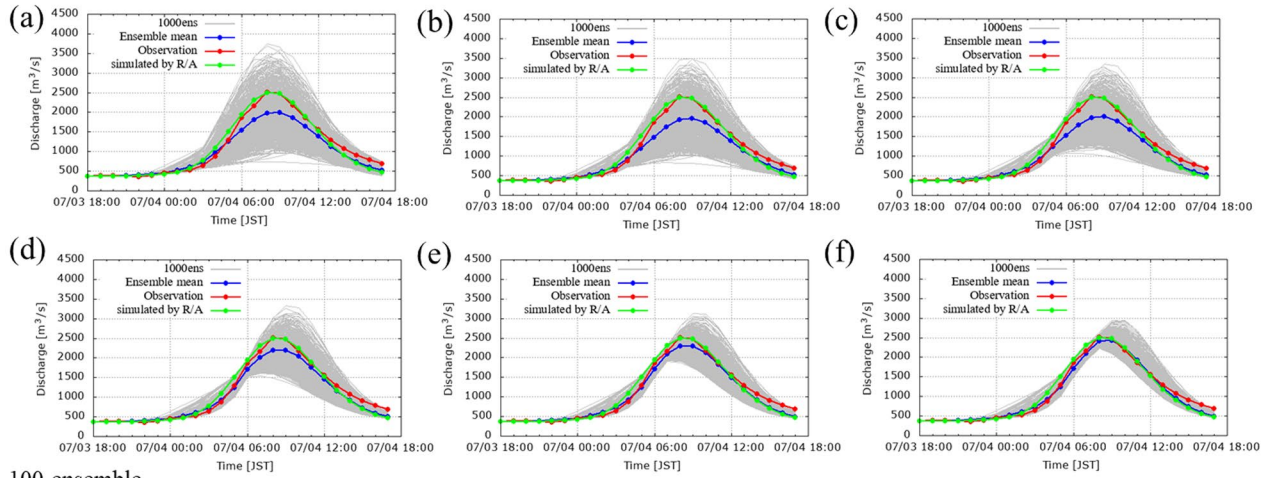


Fig. 17 Application of the Kalman filter on the discharge simulations of 21, 100 and 1000 ensembles for Ichifusa dam (a–g): The Kalman filter was applied until: **a** 11, **b** 12, **c** 13, **d** 14, **e** 15 and **f** 16 h

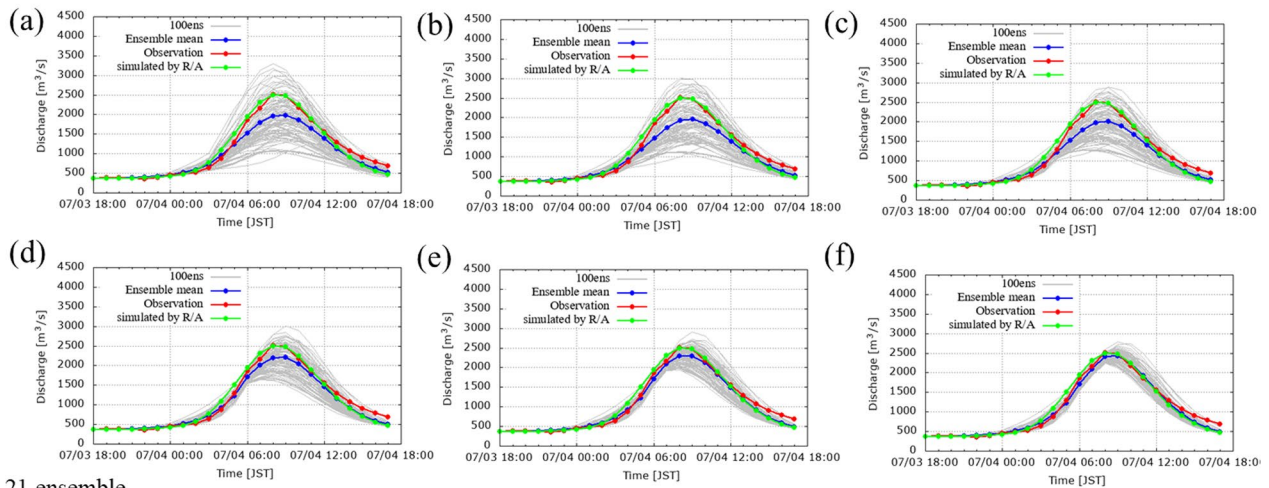
the inundation beyond the observation (i.e., simulated by R/A without dams) did not differ much between selected 1–100, 1–200, 1–500 and 1–1000 member

ensembles. In other words, the number of ensemble members could be reduced in case of 2.5-dimensional inundation predictions unlike the three-dimensional

1000 ensemble



100 ensemble



21 ensemble

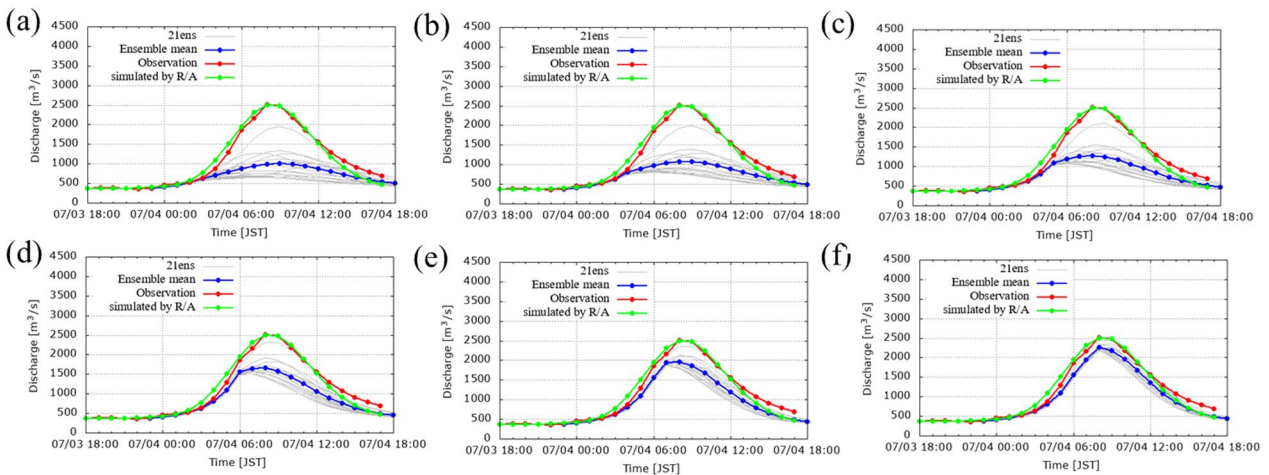


Fig. 18 Application of the Kalman filter on the discharge simulations of 21, 100 and 1000 ensembles for Kawabegawa dam (a–g): The Kalman filter was applied until: **a** 11, **b** 12, **c** 13, **d** 14, **e** 15 and **f** 16 h

weather/rainfall simulations, although finding out the proper number of ensemble members remained as the future work.

Abbreviations

| | |
|-------|---|
| LETKF | Local Ensemble Transform Kalman Filter |
| NWPs | Numerical Weather Predictions |
| JMA | Japan Meteorological Agency |
| EPS | Ensemble Prediction System |
| GEPS | JMA's Global Ensemble Prediction System |
| MEPS | JMA's Mesoscale Ensemble Prediction System |
| ECMWF | European Centre for Medium-Range Weather Forecasts |
| SCALE | Scalable Computing for Advanced Library and Environment |
| COSMO | Consortium for Small-scale Modeling numerical weather forecasting model |
| NHM | JMA nonhydrostatic model |
| FSS | Fractions Skill Score |
| RRM | Rainfall–runoff model |
| SFM | Storage function model |
| SWE | Shallow water equation |
| R/A | JMA's radar–raingauge rainfall |
| GSI | Geospatial Information Authority of Japan |

Acknowledgements

The first author joined the investigation committee for the Kumagawa River flooding on July 4, 2020, by the Japan Society of Civil Engineers headed by Prof. Omoto from Kumamoto University. Through the activity, we have received useful comments and hydrological data from the Kumamoto Prefecture, Ministry of Land, Infrastructure, Transport and Tourism (MLIT) and JMA. The authors would like to thank them.

Author contributions

KK conceptualized the entire research work in hydrology, carried out flood simulations, made the figures/tables and wrote many parts of the paper. LD carried out the 1000 ensemble weather simulations and wrote the meteorological summary in the paper, TK took the leading role in the research of the meteorological part, TA worked together with KK for many parts of hydrological research, TO supported 1000 ensemble flood simulations using a supercomputer, KS advised the research, especially the meteorological part, DN carried out physically based rainfall–runoff simulation which was used as a benchmark for the rainfall–runoff simulation by SFM, and TS advised in many aspects of the hydrological research. All authors read and approved the final manuscript.

Funding

This research used computational resources of the supercomputer Fugaku and other computers of the High Performance Computing Infrastructure (HPCI) system provided by the RIKEN R-CCS (ID:hp200128, hp210166, hp220167) supported by MEXT (JPMXP1020200305) as "Program for Promoting Researches on the Supercomputer Fugaku" (Large Ensemble Atmospheric and Environmental Prediction for Disaster Prevention and Mitigation). Likewise, this work was supported by JSPS KAKENHI Grant Number 19K04618.

Availability of data and materials

JMA-NHM is available under the collaborative framework between the Meteorological Research Institute (MRI) of Japan and related institutes or universities. Likewise, the DRR and SWE models are available under the collaborative framework between Kobe University and related institutes or universities. The meteorological data and hydrological data were provided by MLIT, Kumamoto Prefecture and JMA. We will consider making other data available upon request. Research cooperation is preferable for data provision.

Declarations

Competing interests

The authors declare that they have no competing interest.

Received: 24 July 2022 Accepted: 21 January 2023
Published online: 02 February 2023

References

- Athans M, Wishner RP, Bertolini A (1968) Suboptimal state estimation for continuous time nonlinear systems from discrete noisy measurements. *IEEE Trans Autom Control* 13(5):504–514
- Duc L, Kuroda T, Saito K, Fujita T (2015) Ensemble Kalman Filter data assimilation and storm surge experiments of tropical cyclone Nargis. *Tellus A*. <https://doi.org/10.3402/tellusa.v67.25941>
- Duc L, Kawabata T, Saito K, Oizumi T (2021) Forecasts of the July 2020 Kyushu heavy rain using a 1000-member ensemble Kalman filter. *SOLA* 17:41–47. <https://doi.org/10.2151/sola.2021-007>
- Duc L, Saito K (2017) A 4D-EnVAR data assimilation system without vertical localization using the K computer. In: Japan Geoscience Union meeting, 20–25 May 2017, Chiba, Japan, AAS12-P04
- Fukuoka district meteorological observatory (2020) Weather report at disaster (free translation), https://www.jma-net.go.jp/fukuoka/chosa/saigai/20200705_fukuoka.pdf. Accessed 30 Jan, 2022
- Geospatial Information Authority of Japan (2020) Information on heavy rainfall of July 2020 (free translation), https://www.gsi.go.jp/BOUSAI/R2_kyusyu_heavyrain_jul.html#9, Accessed 30 Jan 2022
- Hanasaki R, Ishitsuka Y, Yamazaki D, Yoshimura K (2019) Implementing reservoir operation in a probabilistic flood forecast system and its application to 2015 Kinu river flood. *J Jpn Soc Civ Eng Ser B1(75):L151-L156*. https://doi.org/10.2208/jscejhe.75.2_L151
- Japan Society for Civil Engineers (JSCE) (2002) Handbook of Hydraulics in Japan (free translation), Chapter 1–11: Storage function model with a Kalman filter (by Akira Kawamura)
- Hoshi K, Yamaoka I (1982) A relationship between kinematic wave and storage routing model. *Proc Jpn Conf Hydraul* 26:273–278. <https://doi.org/10.2208/prohe1975.26.273>
- Japan Meteorological Agency (2021) Numerical Weather Prediction Description, Chapter: Ensemble Weather Prediction (free translation since it is written in Japanese), <https://www.jma.go.jp/jma/kishou/books/nwpa/isetu/nwpa/isetu.html> Accessed 3 Mar, 2022
- Kawabata T, Ueno G (2020) Non-Gaussian probability densities of convection initiation and development investigated using a particle filter with a storm-scale numerical weather prediction model. *Mon Wea Rev* 148:3–20. <https://doi.org/10.1175/MWR-D-18-0367.1>
- Kawamura A, Jinno K, Oshikawa M, Ueda T, Nakayama H (1993) Real time optimal control of an estuary barrage gate by use of the self-control tuning control theory. *J Jpn Soc Civ Eng Ser B1 (Hydraulic Engineering)*, No.461/II-22, pp. 11–20
- Kinki district of maintenance station, Ministry of Land, Infrastructure, Transport and Tourism (2020) First report for the committee on heavy rainfall of July 2020 at Kumagawa river (free translation), http://www.qsr.mlit.go.jp/yatusiro/site_files/file/bousai/goukensho/20200825shiryou1.pdf, 2020. Accessed 30 Jan 2022
- Kobayashi K, Otsuka S, Saito K (2016a) Ensemble flood simulation for a small dam catchment in Japan using 10 and 2 km resolution nonhydrostatic model rainfalls. *Nat Hazards Earth Syst Sci* 16:1821–1839. <https://doi.org/10.5194/nhess-16-1821-2016>
- Kobayashi K, Kitamura D, Ando K, Ohi N (2016b) Parallel computing for high-resolution/large-scale flood simulation using the K supercomputer. *Hydrol Res Lett* 9(4):61–68. <https://doi.org/10.3178/hrl.9.61.2016>
- Kobayashi K, Duc L, Apip, Oizumi T, Saito K (2019) Ensemble flood simulation for a small dam catchment in Japan using nonhydrostatic model rainfalls: part 2: flood forecasting using 1600-member 4D-EnVar-predicted rainfalls. *Nat Hazards Earth Syst Sci*. <https://doi.org/10.5194/nhess-2018-343>
- Kobayashi K, Duc L, Apip, Oizumi T, Saito K (2020) Ensemble flood simulation for a small dam catchment in Japan using nonhydrostatic model rainfalls: part 2: flood forecasting using 1600-member 4D-EnVar-predicted rainfalls. *Nat Hazards Earth Syst Sci* 20:755–770. <https://doi.org/10.5194/nhess-20-755-2020>
- Kunii N (2014) The 1000-member ensemble kalman filtering with the JMA nonhydrostatic mesoscale model on the K computer. *J Met Soc Japan* 92:623–633. <https://doi.org/10.2151/jmsj.2014-607>

- Nash JE, Sutcliffe V (1970) River flow forecasting through conceptual models part I: a discussion of principles. *J Hydrol* 10:282–290. [https://doi.org/10.1016/0022-1694\(70\)90255-6](https://doi.org/10.1016/0022-1694(70)90255-6)
- Necker T, Geiss S, Weissmann M, Ruiz J, Miyoshi T, Lien GY (2020) A convective-scale 1000-member ensemble simulation and potential applications. *Quart J Roy Meteor Soc* 146:1423–1442. <https://doi.org/10.1002/qj.3744>
- Nohara D, Sumi T (2022) Reservoir operation against large-scale floods due to Typhoon Hagibis and applicability of ensemble forecast to preliminary release. *J JSCE* 10:275–287
- Nohara D, Kitani K, Michihiro Y, Sumi T (2020) Applicability of ECMWF Medium-range Ensemble Rainfall Forecast to prior release operation of a hydro-power dam. *J Jpn Soc Civ Eng Ser B1* 76(2):829–834
- Oizumi T, Kawabata T, Duc L, Kobayashi K, Saito K, Ohta T (2022) Flood forecasting using 1000-member ensemble prediction for a severe flood event, Japan Geoscience Union Meeting 2022 Abstract, AAS05-05. https://www.jpgu.org/meeting_e2022/program.php
- Ono KM, Kunii YH (2021) The regional model-based mesoscale ensemble prediction system, MEPS, at the Japan Meteorological Agency. *Q J J Meteor Soc* 147:465–484
- Roberts NM, Lean HW (2008) Scale-selective verification of rainfall accumulations from high-resolution forecasts of convective events. *Mon Wea Rev* 136:78–97
- Sayama T, Yamada M, Sugawara Y, Yamazaki D (2020) Ensemble flash flood predictions using a high-resolution nationwide distributed rainfall-runoff model: case study of the heavy rain event of July 2018 and Typhoon Hagibis in 2019. *Prog Earth Planet Sci* 7:75. <https://doi.org/10.1186/s40645-020-00391-7>
- Sumi T, Nohara D (2020) Report on Kumagawa river flood on July 2020 (focusing on the Ichifusa dam and Kawabegawa dam), http://ecohyd.dpri.kyoto-u.ac.jp/content/files/DisasterSurvey/2020/report_KumaRiverFloods2020_v3.pdf. Accessed 30 Jan, 2022
- Ueda T, Kawamura A, Jinno K (1984) Detection of abnormality by the adaptive Kalman filter. *J Jpn Soc Civ Eng Ser B1* (345):111–121
- Yamaguchi H, Ikebami M, Iwahira T, Ochi K, Sekiguchi R, Takakura T (2021) Upgrade of JMA's Global Ensemble Prediction System, CAS/JSC WGNE Res. *Act Atmos Ocea Modell* 52:12–13

Publisher's Note

Springer Nature remains neutral with regard to jurisdictional claims in published maps and institutional affiliations.

Submit your manuscript to a SpringerOpen[®] journal and benefit from:

- Convenient online submission
- Rigorous peer review
- Open access: articles freely available online
- High visibility within the field
- Retaining the copyright to your article

Submit your next manuscript at ► [springeropen.com](https://www.springeropen.com)
